Proteomic and Post-Translational Modification Profiling of Exosome-Mimetic Nanovesicles Compared to Exosomes

Kenari, Amirmohammad Nasiri; Kastaniegaard, Kenneth; Greening, David W; Shambrook, Mitch; Stensballe, Allan; Cheng, Lesley; Hill, Andrew F

Published in:
Proteomics

DOI (link to publication from Publisher):
10.1002/pmic.201800161

Publication date:
2019

Document Version
Accepted author manuscript, peer reviewed version

Exosome-mimetic nanovesicles contain distinct proteome and post-translational modified protein cargo, in comparison to exosomes

Amirmohammad Nasiri Kenari[#1], *Kenneth Kastaniegaard*[#2], *David W. Greening*[1], *Mitch Shambrook*[1], *Allan Stensballe**[2], *Lesley Cheng*[1] *and Andrew F. Hill**[1]

[1]*Department of Biochemistry and Genetics, La Trobe Institute for Molecular Science, La Trobe University, Australia*

[2]*Department of Health Science and Technology, Faculty of Medicine, Aalborg University, Denmark*

*Authors to whom correspondence should be addressed: andrew.hill@latrobe.edu.au and as@hst.aau.dk

#Amirmohammad Nasiri Kenari and Kenneth Kastaniegaard contributed equally to this work

Keywords: Exosomes, extracellular vesicles, therapeutic exosomes, mimetic-nanovesicles, artificial extracellular vesicles, proteomics, post-translational modification

Received: 07 31, 2018; Revised: 02 17, 2019; Accepted: 02 18, 2019

This article has been accepted for publication and undergone full peer review but has not been through the copyediting, typesetting, pagination and proofreading process, which may lead to differences between this version and the Version of Record. Please cite this article as doi: 10.1002/pmic.201800161.

Running title: Proteome of mimetic-nanovesicles

ABSTRACT

Cargo sorting of selective biomolecules and relatively low quantities of extracellular vesicles (EVs) produced by cells present challenges when upscaling EV production for therapeutic use. These issues may be overcome through producing artificial EVs. Cell-derived mimetic nanovesicles (M-NVs) are a potentially promising alternative to EVs for clinical applicability, demonstrating cost-effectiveness and higher yield without incumbent production and isolation issues. Although several studies have shown that M-NVs have similar morphology, size and therapeutic potential compared to exosomes, comprehensive characterization and to what extent M-NVs components mimic exosomes remain elusive. We generated M-NVs through the extrusion of cells and performed proteomic profiling which defined proteins associated with membrane and cytosolic components. In this context, our proteomic data reveal a subset of proteins that are highly abundant in M-NVs in comparison to exosomes. M-NVs contain proteins that largely represent the parental cell proteome, whereas the profile of exosomal proteins highlight their endosomally derived origin. This advantage of M-NVs alleviates the necessity of endosomal sorting of endogenous therapeutic proteins or RNA into exosomes. Our study also highlights differences in protein post-translational modifications among M-NVs, as distinct from exosomes, using a non-targeted informatic approach, specifically showing phosphorylation, ubiquitination, and thiophosphorylation as enriched protein modifications in M-NVs. Overall this study provides key insights into defining the proteome composition of M-NVs as a distinct from exosomes, and the potential advantage of M-NVs as an alternative nanocarrier when spontaneous endosomal sorting of therapeutics are limited.

1 INTRODUCTION

Exosomes are cell-derived extracellular vesicles (EVs) of endosomal origin that are naturally released by most cells and are fundamental for intercellular communication [1]. Exosomes are produced through further modification and enrichment at multi-vesicular bodies (MVBs), resulting in enrichment of proteins associated with the endosomal pathway. They have the ability to transport endogenous biological cargo, such as small RNAs, mRNAs and proteins across neighboring and distant cells. This feature of exosomes as natural mediators of intercellular communication opens the avenue for utilizing them as a therapeutic delivery system. Many researchers have manipulated the architecture of exosomes by genetically engineering specific proteins or peptides to further enhance therapeutic efficiency [2]. Exosomes offer significant advantages over conventional lipid-based delivery systems including biocompatibility, stability, low immunogenicity and innate ability to target and interact with recipient cells. However, translation to clinical applications has been limited by several factors such as heterogeneity, cargo sorting, therapeutic loading, large-scale manufacture, low yield, storage, cost and multi-step approaches in isolation and purification [3-9]. To address these challenges an alternative approach has been employed to generate an artificial vesicle to mimic EVs (mainly exosomes) by morphology, size and potentially *in vitro* and *in vivo* behavior. Cell-derived mimetic nanovesicles (M-NVs) are an emerging and potentially promising alternative to exosomes for clinical applicability, demonstrating reproducibility in protocol, cost-effectiveness and higher yield production rates. The benefits of M-NVs address issues of relatively low quantities of exosomes produced by cells and the involvement of extensive isolation and purification procedures [10-14]. Importantly, the biological activity and uptake of M-NVs was confirmed *in vitro* using cellular uptake studies and *in vivo* biodistribution studies. Similar to exosomes, proteins on the surface of M-NVs may be involved in signaling and ultimately the fate of vesicles. The membrane proteins found on M-NVs were shown to be important in the efficient delivery of doxorubicin as trypsinization of M-NVs imped their function. This suggests that membrane proteins found on the surface of M-NVs play a crucial role in vesicle uptake [13].

M-NVs can be loaded with therapeutics by genetically engineering the cell or exogenously using electroporation or during the extrusion of cells [11, 15]. M-NVs generated from monocytes or macrophages exogenously loaded with a chemotherapeutic compound by electroporation was shown to be successfully delivered *in vivo* to malignant tumors [13] and demonstrated comparable delivery

efficiency to exosomes. Unlike exosomes, which requires selective sorting of cargo through the endosomal pathway, it's feasible to engineer cells to overexpress cytosolic or membrane proteins or RNA and subsequently generate M-NVs. For example, expressing a shRNA of interest into a parental cell line was shown to produce M-NVs packaged with siRNA that could knock down c-Myc [11]. A recent study demonstrated successful packaging of Lnc-RNA-H19 into M-NVs targeted for wound healing in diabetics through expressing Lnc-RNA-H19 in parental cells [15]. Other examples in the literature include packaging M-NVs with paclitaxel during the extrusion process that was used to deliver anti-cancer drugs to target cells [16]. M-NVs derived from murine pancreatic β-cell line were able to differentiate therapeutic insulin producing cells providing a cell free therapeutic approach [12]. The regenerative capability of M-NVs may be useful in replacing cell-based therapeutics where the targeted tissues may require enhanced potency which could be further enriched within M-NVs.

Although the therapeutic potential of M-NVs has been demonstrated, the proteome cargo of M-NVs has not been comprehensively characterized and it is unknown to what extend their cargo could mimic the proteome of natural exosomes. Furthermore, it is imperative to comprehensively characterize their composition as their contents may potentially have an effect on recipient cells. In this study, we investigated the proteome of M-NVs that can be produced through the extrusion of cells and compared the profiles to exosomes secreted from the same cell line. We report a subset of proteins highly abundant in M-NVs in comparison to well-known exosomal cargo proteins. Given the importance of protein modifications in exosome biology, we further investigated the protein post-translational modification (PTMs) profile among M-NVs and exosomes using a non-targeted informatic approach, highlighting unique differences in M-NVs. Using M-NVs would address current challenges faced with efficient loading of therapeutics to exosomes. Collectively, this study provides key insights into defining the proteome composition of M-NVs as distinct from exosomes, and further understanding of the emerging potential of M-NVs as an alternative nanocarrier modality for loading therapeutics which are not naturally sorted into exosomes.

2 MATERIALS AND METHODS

2.1 Cell culture

Human neuroblastoma SH-SY5Y cells were purchased from American Type Culture Collection (ATCC). To generate M-NVs, SH-SY5Y cells were maintained in complete Dulbecco's Modified Eagle Medium (DMEM; Invitrogen) supplemented with 10% (v/v) heat inactivated fetal calf serum (FCS; Invitrogen) and 5% (v/v) GlutaMAX^{TM} (Invitrogen) which were incubated at 37° C in 5% CO_2. For exosome isolation, cells were grown to ~90% confluency and passaged by resuspending in 10% exosome-depleted FCS (ultracentrifuged at 100,000 g for 16 h at 4° C) DMEM and left to culture at 37° C with 5% CO_2 for 48 h.

2.2 Exosome isolation by differential ultracentrifugation

Exosome isolation from conditioned media was performed using differential ultracentrifugation as previously described [17]. Briefly, culture medium (CM) (120 mL from approximately 1.2×10^8 cells) was harvested and centrifuged (2,000 *g*, 10 min) to sediment dead cells and remove cellular debris. CM was centrifuged at 10,000 *g* for 30 min to remove large microvesicles. The resultant supernatant was ultracentrifuged at 100,000 g for 70 min at 4° C to pellet exosomes. The exosome pellet was resuspended in 1 mL filtered (0.2 μm) DPBS (Dulbecco's Phosphate-Buffered Saline, Invitrogen), and centrifuged at 100,000 g for 70 min at 4° C and resuspended in DPBS.

2.3 M-NVs generation and purification

SH-SY5Y cell-derived mimetic nanovesicles (M-NVs) were generated by a Mini-Extruder system (Avanti Polar Lipids) following a previously published protocol [13]. Cells (~90% confluency, 1.2×10^8 cells) were harvested and re-suspended in filtered DPBS. M-NVs were generated from a suspension of cells through sequential filtration using polycarbonate track-etched membranes of 10 μm, 5 μm and 1 μm filters (Whatman membrane filter, Merck) which involved passing the suspension 13 times across each filter. The extruded M-NVs were subsequently purified using OptiPrep™ density gradient. Briefly, to prepare the discontinuous iodixanol gradient, 50% (w/v) and 10% (w/v) solutions of iodixanol were made by diluting a stock solution of OptiPrep™ (60% (w/v) aqueous iodixanol

from Axis-Shield PoC, Norway) with 10X NTE buffer (100 mM Tris, 10 mM EDTA and 1.37 M NaCl, pH 7.4). The gradient was formed by adding 1 mL of 50% (v/v) iodixanol solution to a 14 × 89 mm polyallomer tube (Microfuge® Tube, Beckman Coulter), followed by careful layering of 1 mL 10% (v/v) solution. For M-NV purification, extruded vesicles (5 mL) were overlaid on the gradient, followed by centrifugation at 100,000 g (45 Ti rotor; Beckman Coulter-Optima XPN-100) for 2 h at 4° C. Seven individual fractions were collected manually (with increasing density) and Coomassie Brilliant Blue R-250 stain used to determine protein abundance on samples resolved using SDS-PAGE. Here, samples were loaded on 4-12 % Bis-Tris SDS-PAGE protein gel (Invitrogen) and resolved at 120 V for 1 h and 20 min. The SDS-PAGE gel was removed from the electrophoresis tank and stained with Coomassie blue stain (10% (v/v) acetic acid, 40% (v/v) methanol and 0.1% (w/v) Coomassie Brilliant Blue R-250 (Sigma-Aldrich) and heated in the microwave for 45 s. The gel was then incubated for 5 min at room temperature on a shaker followed by destaining buffer (10% (v/v) acetic acid, 20% (v/v) methanol) and heated in the microwave for 45 s. Images were taken by ChemiDoc™ Touch Imaging System (Bio-Rad). The protein content of exosomes and M-NVs preparations was estimated by Pierce™ BCA protein assay kit (ThermoFisher).

2.4 Western immunoblotting

Following SDS-PAGE, proteins were transferred to a 0.45 μm polyvinylidene fluoride (PVDF) membrane using Bio-Rad western transfer apparatus in transfer buffer (25 mM Tris, 200 mM glycine, 20% (v/v) methanol) at 100 V for 50 min. The membrane was then blocked with 5 % (w/v) skim milk and incubated with primary antibodies overnight at 4° C . Membranes were washed and probed with secondary antibody for 1 h at room temperature. The blot was developed by Clarity™ ECL reagent (Bio-Rad) according to the manufacturer's protocol. The membranes were imaged by ChemiDoc Touch imaging system (Bio-Rad) and further analyzed by Image Lab Software (Bio-Rad). Primary antibodies used for western blot analysis were TSG101 (Abcam), Flotillin (BD Bioscience), Bcl2 (BD Bioscience), Actin (Cell Signaling Technology) and Mouse secondary antibody (GE Healthcare).

2.5 Silver staining

Gel-based protein profiles for cell lysate, exosomes and M-NVs was assessed using silver staining (SilverQuest™ Silver staining kit, Invitrogen). Samples were loaded on 4-12 % Bis-Tris SDS-PAGE

protein gel (Invitrogen) and resolved at 120V for 1 h and 20 min. The gel was gently rinsed with ultrapure water and stained according to the manufacturer's protocol.

2.6 Nanoparticle tracking analysis

Particle size and concentration were measured by NanoSight NS300 (Malvern Panalytical). Samples were diluted with DPBS, loaded in a 1 mL syringe and analyzed with the infusion rate of 50. The movement of particles through the flow cell was recorded for 30 s and five technical replicates performed. Analysis was carried out by the NanoSight NS300 NTA software (NTA 3.2). Four biological replicates were performed for both vesicle types.

2.7 Transmission electron microscopy

Heavy carbon-coated formvar copper grids (ProSciTech, SA, Australia) were glow discharged and incubated with an aliquot of exosomes and M-NVs for 15 min at room temperature. Grids were washed with ultra-pure water and negatively stained with 2.5 % (v/v) uranyl acetate (Agar Scientific). Excess solution was blotted off immediately and samples were allowed to dry for 15 min prior to imaging. Electron microscopy (EM) images were taken using a Jeol JEM-2100 instrument.

2.8 Mass spectrometry-based proteomics

M-NVs, exosomes, and cell lysates were prepared for proteome profiling as described [18]. Briefly, M-NVs (20 μg) and exosomes (20 μg), were lysed in 100 mM triethylammonium bicarbonate in 0.1% Rapigest (Waters, Milford, MA) with 2 min sonication and incubation at 95 °C for 5 min. Cell lysates (20 μg) were lysed in 0.5% sodium deoxycholate in 100 mM triethylammonium and incubation at 95° C for 5 min. Samples were reduced with 12.5 mM tris(2-carboxyethyl)phosphine hydrochloride (Sigma-Aldrich, C4706) at 28° C for 4 h with gentle rotation, alkylated with 12.5 mM chloroacetamide (Sigma-Aldrich) for 30 min at 37° C, and digested with 2 μg bovine sequencing grade trypsin (Promega, V5111) at 37° C for 18 h. For cell lysate samples, sodium deoxycholate was removed following digestion as previously described [19]. Subsequently, peptides were purified and extracted using reverse-phase C18 StageTips (Sep-Park cartridges, Waters, MA) in 85% (v/v)

acetonitrile (ACN) in 0.5% (v/v) formic acid (FA). Peptides were lyophilized and acidified with buffer containing 0.1% FA, 2% ACN.

Proteomic experiments were performed in biological quadruplicates (N=4), with technical replicates (N=3), with MIAPE-compliance [20, 21]. A peptide pool was made group-wise using 2 µl from each sample. Samples were then analyzed per LC-MS analysis, in random and duplicates of the pooled sample distributed, so a pool was analyzed every seventh run. A nanoflow UPLC instrument (Ultimate 3000 RSLCnano, Thermo Fisher Scientific) was coupled on-line to a Q-Exactive HF Orbitrap mass spectrometer (Thermo Fisher Scientific) with a nanoelectrospray ion source (Thermo Fisher Scientific). Peptides were loaded (Acclaim PepMap100, 5 mm × 300 µm i.d., µ-Precolumn packed with 5 µm C18 beads, Thermo Fisher Scientific) and separated (Acclaim PepMap RSLC C18 column 1.9 µm 120Å, 360/75 µm × 750 mm, Thermo Fisher Scientific) with a 60 min gradient (M-NVs/exosomes) and 90 min gradient (cell lysates) from 4-50% (v/v) phase B (0.1% (v/v) FA in 80% (v/v) ACN) (4–10% from 0–10 min, 10–50% from 10–60 min (M-NVs/exosomes) and 10-90 min (cell lysates) at a flow rate of 300 nL/min operated at 60° C .

The mass spectrometer was operated in positive, data-dependent mode where the top 6 most abundant precursor ions in the survey scan (350–1500 m/z) (standard sample) and top 15 most abundant precursor ions in the survey scan (350–1500 m/z) (pooled sample) was used for MS/MS fragmentation. Survey scans were acquired at a resolution of 60,000 with MS/MS resolution of 15,000. Unassigned precursor ion charge states and singly charged species were rejected and peptide match disabled. The isolation window was set to 1.6 Da and selected precursors fragmented by HCD with normalized collision energies of 27 with a maximum ion injection time of 110 msec. Ion target values were set to 3e6 and 1e5 for survey and MS/MS scans, respectively. Dynamic exclusion was activated for 6 sec. Data was acquired using Xcalibur software v4.0 and Tune 2.9 (Thermo Fisher Scientific). Raw mass spectrometry data is deposited in the ProteomeXchange Consortium via the PRIDE partner repository with the dataset identifier [22]

2.9 Database searching and protein identification

For protein identification, the MS raw-files of the samples and pooled samples were searched in MaxQuant [23];v1.5.8.3 using standard setting including match-between-runs against UP000005640 Homo sapiens (Uniprot proteome reference; 2/22/2017, 20.347 proteins) and reversed database for FDR investigation. Cell lysates were searched independently from the M-NV and exosomes samples. Peptide lists were generated from a tryptic digestion with up to two missed cleavages, cysteine carbamidomethylation as fixed modification, and methionine oxidation and protein N-terminal acetylation as variable modifications. Data was analyzed with a parent tolerance of 4.5 ppm, fragment tolerance of 20 ppm and minimum peptide length 7, with false discovery rate 1% at the peptide and protein levels, and with label-free quantitation (LFQ) [24]. The output was processed using R Programme. Reverse identifications were excluded, and non-zero quantitation values required in more than half of each sample group for further processing.

LFQ data was filtered for two or more unique peptides and log2-transformed. Principle component analysis (PCA) including all sample groups was performed, where multivariate imputation by chained equations using predictive mean matching was used for missing values [25]. Relative quantification comparison between M-NV and exosomes was performed in R, where all data were included and filtered. Technical replicates were averaged and hierarchical clustering analyses (HCA) performed, missing values computations performed as described. For differential expression analyses between groups, unpaired two-tailed t-tests and resulting p-values were adjusted by the Benjamini-Hochberg multi-test adjustment method for a high number of comparisons [26] and statistics performed as previously described [18, 21]. For gene ontology (GO) enrichment and pathway analyses, FunRich [27]; v3.1.3, Kyoto Encyclopedia of Genes and Genomes (KEGG) and NIH Database for Annotation, Visualization and Integrated Discovery Bioinformatics Resources 6.7 (DAVID) resources were utilized using recommended analytical parameters [28]. For gene ontology enrichment and network analyses UniProt (www.uniprot.org) database resource (biological process, molecular function) was utilized.

2.10 Protein post-translational modifications identification and quantitation data analysis

To identify global PTMs differences raw data (M-NVs/exosomes) was searched using PEAKS ([29]; v8.5) against the UP000005640 *Homo sapiens* Uniprot database. Initially, for protein and PTM identifications, all standard settings were employed with carbamidomethyl (C) as a static modification

and oxidation (M) as variable modifications. The most abundant modification was then searched separately in database searches as variable modifications to ensure full coverages. All modifications were restricted to a false discovery rate 1% at the peptide and protein levels and annotation score (A) > 20 [29]. LFQ modification outputs were combined and processed as described using R, with contaminants, and reverse identification excluded from further data analysis. LFQ ratio between modified and unmodified peptides was calculated and log2 transformed as well as non-zero quantitation value in more than half of the samples was required for further analysis. Resulting p-values were adjusted by the Benjamini-Hochberg multi-test adjustment method for a high number of comparisons [26] and statistics performed as previously described [30]. HCA analysis was made on the averaged technical replicates, and missing values was dealt with using same procedure as the data-dependent proteome profiling protein identification. Significant differences between the two groups were found using the same procedure as for the protein quantification data. Proteins with significant regulated PTMs corresponding to a 2-fold change and adjusted p-value of <0.05 was cross validated for identification with a MaxQuant PTM search of the top 11 modifications, a MaxQuant Dependent peptide search and a literature search. Six MaxQuant searches was performed with the different modifications as variable modifications: 1: Acetylation (N-term) and Deamidation (NQ) 2: Dimethylation(KR) and Methylation(KR) 3: methionine oxidation and Sulfation 4: Phosphorylation (STY) 5: Pyro-glu from E, Pyro-glu from Q 6: Carbamylation and Ubiquitination. Otherwise the same settings as mentioned earlier was applied. Same setting was used in MaxQuant Dependent peptide with oxidation as variable modification and Dependent peptide search FDR set to 0.01 together with a mass bin size of 0.0065 Dalton.

3 RESULTS AND DISCUSSION

In this study, we generated M-NVs by extruding human neuroblastoma SH-SY5Y cells which were then characterized for EV markers and directly compared to SH-SY5Y exosomes. Label-free proteomics was then performed to investigate the proteome between M-NVs and exosomes to provide an insight into what extent M-NVs mimic the proteome of biological exosomes.

3.1 Production of Cell-derived M-NVs and Isolation of exosomes

To obtain cell-derived M-NVs and exosomes, SH-SY5Y cells were harvested to generate M-NVs, while exosomes were isolated from the conditioned supernatant (**Figure 1**). For M-NVs, cells (1.2 ×

10^8) were serially extruded through a series of polycarbonate membranes with pore sizes of 10, 5, and 1 μm to generate crude M-NVs (**Figure 1A**). The extruded vesicles were further purified based on two-step OptiPrep density-gradient ultracentrifugation (10 and 50% (v/v) iodixanol) to remove aggregates and heterogenous particles. M-NVs were found enriched in fraction 6 (F6) at the interface of the iodixanol layer. Exosomes were isolated from cell conditioned medium by differential ultracentrifugation and used for subsequent analysis (**Figure 1B**). In order to isolate a sufficient yield of exosomes, a large quantity of cells is required, which involves upscaling cultures for a minimum of 2-3 passages, in addition to an incubation phase of 48 h. Furthermore, exosomes must be depleted from FCS to avoid cross-species contamination of FCS-derived exosomes in the conditioned supernatant. In contrast, generation of M-NVs only requires one passage of cell culture, does not require incubation of exosome-depleted FCS thus, providing a highly efficient system (minimum ~3-4 days saved).

3.2 Characterization of Mimetic NVs and exosomes

Nanoparticle tracking analysis of the purified M-NVs showed a size distribution and a mode of ~186 nm, comparable to that of exosomes (mode ~179 nm) from SH-SY5Y cells (**Figure 2A**). The morphology and shape of purified M-NVs and exosomes was examined using EM to reveal that they were enclosed with a lipid membrane, round cup-shaped vesicles and the preparations were devoid of the parent cells and cellular debris (**Figure 2B**). We observed that from the same number of cells (1.2×10^8) cultured for 24 h, M-NVs produced 3,615 μg of total protein and 5.3×10^{11} particles which was significantly more compared to exosomes which produced 83.5 μg of total protein and 4.7×10^9 particles (**Figure 2C**). Producing M-NVs through serial extrusion increased the yield of total protein by more than 40-fold (average) and particle number more than 100-fold higher (average) than that of naturally produced exosomes from the same parental cells. The results demonstrated here show that producing M-NVs is highly reproducible and allows for large scale production of vesicles as published previously by other groups [11-13].

A challenge in using exosomes as therapeutic delivery system is the lack of standardization for quantification. Currently, a common method for quantification of exosomes is based on cell equivalent or total particles count which is not a definite representation of homogeneity and particle yield. While, the quantification of M-NVs could be reflected by an actual count of particles generated.

In addition, the quantity and composition of exosomes can be influenced by variations in cell physiological behavior. Cell cultures need to be controlled during every passage to ensure that they do not alter the cargo of exosomes and therapeutic potency [31]. The advantages of using cell-derived M-NVs allows for a larger scale production of vesicles from a continuously maintained cell system that is not limited by alterations in cell biology.

3.3 Proteomic profiling reveals distinct protein landscape in M-NVs

To gain insights into the proteome of M-NVs and how their contents compare to the parental cell and biological exosomes, we performed label-free mass spectrometry-based proteomics. Protein visualization using Silver Protein Stain indicates differences in M-NVs in comparison to exosomes and parental cells (**Figure 3A**). Furthermore, we validated and compared the expression of exosomal enriched proteins in M-NVs (**Figure 3B**). TSG101, a protein involved in exosomes biogenesis, is known to be highly enriched in exosomes as seen in Figure 3B. Interestingly, we found that M-NVs do not abundantly package TSG101 which was found to be similar to parental cells. However, flotillin, a membrane associated protein, is found equally expressed in all samples. The expression of membrane associated proteins such as tetraspanins (CD63, CD9 and CD81) have also been found in M-NVs [12, 13] which highlights that the ultrastructure of parental cells and potentially exosomes are conserved at the membrane of M-NVs. Next, we investigated the expression of proteins which are globally present in cells but not selectively sorted into exosomes. While Bcl2 is regarded as a negative marker for exosomes [32, 33], M-NVs were found to contain an abundant amount of Bcl2 protein (**Figure 3B**). Because the overexpression of Bcl2 has been shown to protect immortalized cells from chemically-induced cell death [34] and together with previous studies reporting a low abundance of the apoptotic inducer, Cytochrome C, in M-NVs [16], it is intriguing to speculate that M-NVs could be useful as potential anti-apoptotic agents. Overall, M-NVs can mimic the ultrastructure of exosomes but do not display an abundance of proteins that are typically involved in exosomes biogenesis.

Proteomic profiling identified a total of 2,454 proteins from M-NVs, 2,141 proteins from exosomes, and 4,073 proteins from parental cells. A number of proteins (1,887) were commonly found in all samples (**Figure 3C** and **Supplementary Table 1**). Importantly, 19, 65 and 1,673 unique proteins were identified in M-NVs, exosomes and cells, respectively, indicating the enrichment of distinct proteins in M-NVs and exosomes (**Figure 3C** and **Supplementary Table 1**). To gain insight into the

potential functions of the enriched proteins in M-NVs, we conducted DAVID Functional Enrichment analysis based on GO and Kyoto Encyclopedia of Genes and Genomes (KEGG). Most proteins uniquely found in M-NVs, were associated with membrane protein and transcription factor GO terms. Proteins found to be exclusive to exosomes were associated with cell adhesion, protein lipid assembly and cytoskeletal protein binding. Interestingly, among 65 unique proteins found in exosomes, we report subsets of proteins (AKT3, DNAJC25, MOSPD2, RNASEH2B, SAT1, SRGAP2B, TECPR2 and TLR8) which has not been identified previously in exosomes (ExoCarta).

Variance within samples was demonstrated in an unsupervised Principal Component Analysis (PCA) (**Figure 3D**), indicating low variance between biological/technical replicates, and a distinct separation between exosomes, M-NVs, and cells. Importantly, the predominant variance in the proteome landscape is derived from differences between M-NVs and exosomes.

3.4 M-NVs proteome is distinct from exosomes

To gain insights into the proteome of M-NVs and how this compares to exosomes isolated from the same cell line, we examined the expression profile of each subset using differential expression based on label free quantification (LFQ). A total of 2,502 proteins were quantifiable in M-NVs and exosomes samples after strict filtering. Variance in protein abundance profiles was compared using Hierarchical clustering (**Figure 4A**), representing a distribution of differentially and similarly expressed proteins in M-NVs and exosomes. Differential protein expression between samples was examined by LFQ, student's t-test and the resulting p-values corrected for multiple testing using the Benjamini-Hochberg procedure, indicating 1,664 proteins were significantly differentially expressed ($FC>2$, $p<0.05$) (**Figure 4B**). Importantly, this differentially regulated protein subset is more than 65% of the quantifiable proteome, highlighting the different origin and composition of cell/plasma membrane-enriched M-NVs in comparison to endosomally-derived exosomes [35] . More specifically, when comparing biological and functional significance of these alterations in the proteome profiles between M-NVs and exosomes based on GO analyses, changes in translation, RNA processing, mRNA splicing, mitochondrial function, and protein transport to membrane were salient changes in M-NVs (**Figure 4C**). MAPK signalling and functions associated with cell proliferation and protein folding, in addition PTMs were enriched in exosomes, and support the known literature of these components associated with exosomes biology [36-38].

To identify enriched proteins present in M-NVs and exosomes, we performed statistical analysis on the expression levels of proteins identified in these data sets. We demonstrated 28 significantly enriched proteins in exosomes and 33 significantly enriched proteins in M-NVs (**Figure 5**). Among the exosomes-enriched conventional markers were proteins involved in the ***E***ndosomal ***S***orting ***C***omplex ***R***equired for ***T***ransport (ESCRT) machinery such as TSG101 [39, 40] vacuolar protein-sorting proteins (VPS4B/13C/28/37B), multivesicular body proteins (CHMP1A/2A/4B/5), proteins involved in co-ordination of intracellular vesicle trafficking (e.g., tetraspanins such as CD9, CD81[41, 42] and small Rab GTPases such as RAB27B and RAB35 [43, 44]) and annexins (ANXA5, ANXA6 [45]) (**Figure 5**). The total number of proteins enriched in exosomes associated pathways was indeed, mostly derived from the exosomes samples (59.6%, **Figure 5**) compared to M-NVs (40.4%, **Figure 5**). This also demonstrates that although M-NVs are not endosomally derived vesicles, to some extend they are enriched in proteins associated with exosomes biogenesis. Of the significantly enriched proteins in M-NVs (57.3% in M-NVs compared to 42.7% in exosomes , **Figure 5**), integral component of membrane (SLC25A4/10/11/13/24, MTCH2, COX4I1, CPT1A, NNT, SFXN3), various NADH dehydrogenase members (NDUFA4/5/10/13, NDUFB9, NDUFS1/2/3/8, and NDUFV1/2) and mitochondrial membrane (SDHB and SFXN1) were identified (**Figure 5**). This finding suggests that significantly upregulated proteins in M-NVs were associated with mitochondrial proteins. A salient finding were several protein translocases, involved in protein transport through plasma and mitochondrial membranes, including mitochondrial import receptor subunit TOM22 (TOMM22) and ADP/ATP translocase 1 (SLC25A4). Several proteins were found to be detected at similar expression levels within M-NVs and exosomes. These shared categories were associated with different pathways and organelles, including: DNA binding (MCM3, MCM4, MCM5 and RECQL), GTP binding (GTPBP1), RNA binding (DDX1/6/39A, PCBP1/2, AIMP1, MARS), mRNA processing (XRN2 and PRPF40A), proteins associated with nucleus (CDK1, KPNA2 and POLR2B) and ribosomal proteins (RPS6/20/23/26 and HNRNPH2). This finding indicates that despite unique packaging of cargos in each vesicle, subsets of proteins in M-NVs and exosomes were found to be expressed at a similar level.

Next, we examined the most abundantly detected proteins in M-NVs. These include mitochondrial membrane proteins (ATP synthases ATP5H/5I/5J, ATPG/K), proteins involved in mitochondrial electron transport (COX5A/5B/41), mitochondrial import (TOM70/TOM22, sideroflexins SFXN1 and SFXN3, MTCH2, and MIRO2), various translocase (ADT1), dehydrogenase (SDHA/B) and synthase

enzymes associated with membrane organisation were ranked as the most abundant top 100 proteins (in comparison to exosomes) (**Supplementary Table 1**). An abundance of NADH dehydrogenase members (NDUA4/5/9, NDUB9, NDUAA/AD, NDUBA, NDUS1/2/3/8, and NDUV1/2) were also found, associated with mitochondrial membrane. Interestingly, Lamina-associated polypeptide 2 members (LAP2A/2B) were also relatively enriched which are important in nuclear transport and organisation, in addition to RNA-binding proteins RBM14, RBM28, and RBMX.

Surface proteins on EVs play a fundamental role in intercellular behavior therefore, we further mined these proteomic data sets for known cell surface and plasma membrane components. We report 158 cell surface, plasma membrane and plasma membrane-associated proteins (**Supplementary Table 2**). These include sodium/potassium-transporting ATPases ATP1A1/A3/B1/B3, plasma membrane-associated small GTPase CDC42 and RALA, paralemmin-1 (PALM) that are involved in plasma membrane dynamics and cell process formation, long-chain fatty acid transport protein 4 (SLC27A4) involved in translocation across the plasma membrane, and phospholipid-transporting ATPase IA (ATP8A1) important in maintenance of asymmetric distribution of the phospholipid bilayer. Further, various integrin components were identified in M-NVs including ITGA1/2/V/6, and ITGB1, and several cell surface receptor proteins were identified, including clusterin (CLU), CD151 and CD63 antigens, myelin protein zero-like protein 1 (MPZL1), plexin-B2 (PLXNB2), and neutral amino acid transporter B(0) (SLC1A5). In addition, various connections between the cytoskeletal network and plasma membrane were identified, including Talin-1 (TLN1) Na(+)/H(+) exchange regulatory cofactor NHE-RF1 (SLC9A3R1), and Ezrin (EZR). Overall, M-NVs contain an abundance of components associated with plasma membrane localization and regulation. These results confirmed that cell-derived M-NVs contain similar, yet distinct protein cargo to exosomes.

In addition to select categories associated with metabolic pathways, mitochondrial function, and integral component of membrane, we observed an enrichment of protein modifications for 88 proteins, including acetylation, phosphoprotein, oxidative phosphorylation, methylation, ubiquinone, and oxidative phosphorylation. Collectively, the bioinformatic analysis of the proteomic content of M-NVs and exosomes revealed potential PTMs that may also be different between M-NVs and exosomes.

3.5 Distinct protein modification profiles of M-NVs and exosomes

Based on significant enrichment of protein modification pathways in M-NVs, and the important role protein modifications play in EV biology, including their roles in exosomes cargo sorting and trafficking [37, 38], we performed unbiased mass spectrometry-based protein (PTM) analysis of M-NVs (**Figure 6A**). In brief, we investigated an informatic approach to identify PTM pattern changes with the requirement of select PTM enrichment that could be identified using discovery-based proteomic data. The ability to identify protein modifications that are both known and novel, shows that this unique informatic PTM approach has the capability to elucidate a greater depth of identification within mass spectrometry discovery datasets, and allow unique insights into the area of protein modification and EV biology.

For global identification of PTMs, M-NVs and exosomes were searched using a denovo based database search engine optimized for PTM detection, BSI PEAKS initially, and subsequently with MaxQuant for protein and PTM identifications against 11 selected protein modifications. For this, individual MaxQuant searches were performed with each distinct modification as well as variable modifications. Using this strategy, 1,829 modified proteins were identified and 1,033 of these were quantified and comparable between the two groups based on Hierarchical clustering analysis, indicating similarity and variance between protein PTM abundance in M-NVs and exosomes (**Figure 6B**).

Between both M-NVs and exosomes, the most commonly identified protein modifications were deamidation of asparagine (N) (22% total) and glutamine (Q) (19% total) (**Figure 6C**) (**Supplementary Tables 2-4**). Deamidation is usually associated with protein degradation and aggregation [46] but have also been suggested to be associated with regulation of the DNA damage response [47]. Deamidation has also been suggested as a result of reactive oxygen species reacting with proteins, as have oxidation of methionine [48] and carbamylation have been linked to enhance the generation of reactive oxygen species [49]. Deamidation of asparagine is a frequent modification occurring as a spontaneous non-enzymatic reaction [50]. This modification is associated with protein degradation [51], and apoptosis in cancer cells [52]. Further, deamidation modifications are often observed in the analysis of mass spectrometry data [53], suggested to result as a consequence of sample preparation which can introduce deamidation [54], yet as samples are treated equally, the chance of significantly regulated artefactual deamination should be limited.

We next aimed to identify select PTMs enriched in M-NVs in comparison to exosomes. Importantly, 216 individual modified proteins were found significantly differentially expressed (21% of total comparable) (student's t-test followed by the Benjamini-Hochberg post-doc procedure, adjusted p-value ≤ 0.05, fold change ≥ 2), while 111 protein PTMs were uniquely identified (6% of total identified) in either M-NVs or exosomes. An important finding was that both known and novel modifications were found to be differentially expressed in M-NVs and exosomes. For enriched protein PTMs in M-NVs, oxidation of methionine (M) (5% total), phosphorylation of serine (S) (2% total), ubiquitination of lysine (K) (8% total), thiophosphorylation of threonine (T) (6% total) and pyroglutamic acid from glutamine (Pyro-glu from Q) (22% total) modifications were predominantly identified beside deamidation (NQ) (**Figure 6C**). These included two known phosphorylation sites (HSPB1 S.82, SPTN1 S.2072) [55, 56] and several proteins with ubiquitination sites, including proteins known to be involved in exosomes biogenesis, cargo selection, and trafficking (YWHAZ K.49, SDCBP S.205) [57, 58]. This is the first report of ubiquitination of SDCBP site S.205. Further, we report ubiquitination of RS27A K.6 and PSMC6 K.369, previously described to be involved in biological processes such as PTMs of proteins and proteolytic activities, respectively [59-62]. In M-NVs there was a unique enrichment of the thiophosphorylation protein modification, in addition to most proteins with pyroglutamic acid from glutamine. Of interest was the thiophosphorylated protein, α-synuclein, which is involved in protein aggregation and neurodegenerative disorders [63]. The aggregation of α-synuclein into mature fibrillar structures is dependent on NAC region spanning residues 61-95 [64]. In our study we report thiophosphorylation on residue 81, however the functional implications of this modification in M-NVs remains to be investigated.

In exosomes, we report phosphorylation (3% total), ubiquitination (2% total), N-terminal protein acetylation (5% total) and methylation (6% total) as determined by automated assignment and high statistical score for site specific assignment (**Figure 6C**). Specifically, significantly upregulated protein phosphorylation sites were identified for HIST1H1B T.4, RPN1 T.39, and SERPINH1 S.53 and Y.55. [65]. Further, two proteins with ubiquitination sites were identified, including the known (VDAC1 K.266) and novel (SCPDH S.208) modifications. Protein N-terminal acetylation and methylation were also identified upregulated in exosomes in comparison to M-NVs. Interestingly, several proteins with methylation modifications in exosomes were associated with RNA binding (FSCN1, GANAB, HS90A, RL9 and RS19) [66]. We report differential protein and protein modifications between exosomes and M-NVs, including significantly enriched ubiquitination of

YWHAZ K.49, PSMC6 K.369 and SDCBP S.205 in M-NVs, while the proteins were significantly upregulated in exosomes. These findings suggest that proteins with and without modifications are distinct between exosomes and M-NVs, highlighting the potential for deubiquitination in exosomal cargo sorting or targeted for inclusion in M-NVs.

Taken together, our unique informatics approach to catalog protein PTMs in M-NVs demonstrated the prevalence of deamidation of asparagine (N) and glutamine (Q) in both M-NVs and exosomes. In exosomes, we report enrichment of protein modifications associated with phosphorylation, ubiquitination, and acetylation, consistent with previous reports of these modifications in vesicle biology and trafficking [67, 68]. Furthermore, our study revealed differences in protein phosphorylation, ubiquitination, and thiophosphorylation among M-NVs, as distinct from exosomes. The functional implications and the reason behind these differences in protein modifications present in M-NVs remains an outstanding question.

The potential value of exosomes as a therapeutic delivery vehicle is increasingly promising, and for many, the safety and feasibility has been demonstrated in clinical trials [69-71]. However, such utility is hampered by complexity, heterogeneity, spontaneous packaging of cargo, production yield of different cells type, cost and timeframe in producing sufficient exosomes for downstream application. Furthermore, as exosomes are endosomally derived vesicles, they are enriched in proteins involved in intracellular assembly and trafficking such as Rab GTPases, annexin and HSP70 which may not be crucial for therapeutic application. Using EV characterization methods and proteomic profiling, this current study provided an insight into M-NVs proteome which is unique from exosomes. Our approach reveals that M-NVs contain distinct proteins associated with protein transport and proteins found at the cell surface in comparison to exosomes. Further, characterization of protein PTMs of M-NVs highlight unique insight into these important protein-specific changes relative to exosomes. Future steps will include the utility of this information to develop reconfigurable therapeutic systems with multiple cell lines. While this study utilized only one cell line, further proteomics analysis of M-NVs generated from different cells could provide further validation of the protein composition of M-NVs, which subsequently could be used for better understanding of M-NVs fusion, uptake as well as *in vitro* and *in vivo* trafficking to further generate engineered M-NVs.

Funding sources

This work was supported by grants from the Australian Research Council (DP170102312 to AFH). ANK is supported by a La Trobe University Postgraduate Scholarship. We acknowledge the La Trobe University-Comprehensive Proteomics Platform for providing infrastructure. The Lundbeck Foundation grant (R247-2017-239) and The Danish National Mass Spectrometry Platform for Functional Proteomics (PRO-MS; grant no. 5072-00007B); the Obel Family Foundation and the Svend Andersen Foundation are acknowledged for parts of this study.

Conflicts of interest

The authors declare no conflict of interest.

4 REFERENCES

[1] M. Colombo, G. Raposo, C. Théry, Annual Review of Cell and Developmental Biology 2014, 30, 255.

[2] L. Alvarez-Erviti, Y. Seow, H. Yin, C. Betts, S. Lakhal, M. J. A. Wood, Nature Biotechnology 2011, 29, 341.

[3] D. Ha, N. Yang, V. Nadithe, Acta Pharm Sin B 2016, 6, 287.

[4] J. Wang, Y. Zheng, M. Zhao, Front Pharmacol 2016, 7, 533.

[5] X. Luan, K. Sansanaphongpricha, I. Myers, H. Chen, H. Yuan, D. Sun, Acta Pharmacol Sin 2017, 38, 754.

[6] L. Barile, G. Vassalli, Pharmacol Ther 2017, 174, 63.

[7] M. S. Kim, M. J. Haney, Y. Zhao, V. Mahajan, I. Deygen, N. L. Klyachko, E. Inskoe, A. Piroyan, M. Sokolsky, O. Okolie, S. D. Hingtgen, A. V. Kabanov, E. V. Batrakova, Nanomedicine 2016, 12, 655.

[8] K. B. Johnsen, J. M. Gudbergsson, M. N. Skov, L. Pilgaard, T. Moos, M. Duroux, Biochim Biophys Acta 2014, 1846, 75.

[9] T. Lener, M. Gimona, L. Aigner, V. Borger, E. Buzas, G. Camussi, N. Chaput, D. Chatterjee, F. A. Court, H. A. Del Portillo, L. O'Driscoll, S. Fais, J. M. Falcon-Perez, U. Felderhoff-Mueser, L. Fraile, Y. S. Gho, A. Gorgens, R. C. Gupta, A. Hendrix, D. M. Hermann, A. F. Hill, F. Hochberg, P. A. Horn, D. de Kleijn, L. Kordelas, B. W. Kramer, E. M. Kramer-Albers, S. Laner-Plamberger, S. Laitinen, T. Leonardi, M. J. Lorenowicz, S. K. Lim, J. Lotvall, C. A. Maguire, A. Marcilla, I. Nazarenko, T. Ochiya, T. Patel, S. Pedersen, G. Pocsfalvi, S. Pluchino, P. Quesenberry, I. G. Reischl, F. J. Rivera, R. Sanzenbacher, K. Schallmoser, I. Slaper-Cortenbach, D. Strunk, T. Tonn, P. Vader, B. W. van Balkom, M. Wauben, S. E. Andaloussi, C. Thery, E. Rohde, B. Giebel, J Extracell Vesicles 2015, 4, 30087.

[10] J.-Y. Wu, A.-L. Ji, Z.-x. Wang, G.-H. Qiang, Z. Qu, J.-H. Wu, C.-P. Jiang, Scientific Reports 2018, 8, 2471.

[11] T. R. Lunavat, S. C. Jang, L. Nilsson, H. T. Park, G. Repiska, C. Lässer, J. A. Nilsson, Y. S. Gho, J. Lötvall, Biomaterials 2016, 102, 231.

[12] K. Oh, S. R. Kim, D.-K. Kim, M. W. Seo, C. Lee, H. M. Lee, J.-E. Oh, E. Y. Choi, D.-S. Lee, Y. S. Gho, K. S. Park, ACS Nano 2015, 9, 11718.

[13] S. C. Jang, O. Y. Kim, C. M. Yoon, D.-S. Choi, T.-Y. Roh, J. Park, J. Nilsson, J. Lötvall, Y.-K. Kim, Y. S. Gho, ACS Nano 2013, 7, 7698.

[14] W. J. Goh, S. Zou, W. Y. Ong, F. Torta, A. F. Alexandra, R. M. Schiffelers, G. Storm, J.-W. Wang, B. Czarny, G. Pastorin, Scientific Reports 2017, 7, 14322.

[15] S.-C. Tao, B.-Y. Rui, Q.-Y. Wang, D. Zhou, Y. Zhang, S.-C. Guo, Drug delivery 2018, 25, 241.

[16] S. Kalimuthu, P. Gangadaran, R. L. Rajendran, L. Zhu, J. M. Oh, H. W. Lee, A. Gopal, S. H. Baek, S. Y. Jeong, S.-W. Lee, J. Lee, B.-C. Ahn, 2018, 9.

[17] L. J. Vella, R. A. Sharples, V. A. Lawson, C. L. Masters, R. Cappai, A. F. Hill, The Journal of Pathology 2007, 211, 582.

[18] H. M. Duivenvoorden, J. Rautela, L. E. Edgington-Mitchell, A. Spurling, D. W. Greening, C. J. Nowell, T. J. Molloy, E. Robbins, N. K. Brockwell, C. S. Lee, M. Chen, A. Holliday, C. I. Selinger, M. Hu, K. L. Britt, D. A. Stroud, M. Bogyo, A. Moller, K. Polyak, B. F. Sloane, S. A. O'Toole, B. S. Parker, J Pathol 2017, 243, 496.

[19] D. N. Nguyen, A. Stensballe, J. C. Lai, P. Jiang, A. Brunse, Y. Li, J. Sun, C. Mallard, T. Skeath, N. D. Embleton, J. E. Berrington, P. T. Sangild, Innate Immun 2017, 23, 524.

[20] S. K. Gopal, D. W. Greening, R. A. Mathias, H. Ji, A. Rai, M. Chen, H. J. Zhu, R. J. Simpson, Oncotarget 2015, 6, 13718.

[21] D. W. Greening, H. Ji, M. Chen, B. W. Robinson, I. M. Dick, J. Creaney, R. J. Simpson, Sci Rep 2016, 6, 32643.

[22] J. A. Vizcaíno, A. Csordas, N. del-Toro, J. A. Dianes, J. Griss, I. Lavidas, G. Mayer, Y. Perez-Riverol, F. Reisinger, T. Ternent, Q.-W. Xu, R. Wang, H. Hermjakob, Nucleic Acids Research 2016, 44, D447.

[23] J. Cox, M. Mann, Nature Biotechnology 2008, 26, 1367.

[24] C. A. Luber, J. Cox, H. Lauterbach, B. Fancke, M. Selbach, J. Tschopp, S. Akira, M. Wiegand, H. Hochrein, M. O'Keeffe, M. Mann, Immunity 2010, 32, 279.

[25] S. van Buuren, K. Groothuis-Oudshoorn, Journal of Statistical Software 2011, 45, 1.

[26] Y. Benjamini, Y. Hochberg, J. R. Stat. Soc. Ser. B-Stat. Methodol. 1995, 57, 289.

[27] M. V. Pathan, V. L. Tagarielli, S. Patsias, Composites Part A: Applied Science and Manufacturing 2017, 93, 18.

[28] W. Huang da, B. T. Sherman, R. A. Lempicki, Nat Protoc 2009, 4, 44.

[29] L. Zhang, D. Li, P. Gao, World Journal of Microbiology and Biotechnology 2012, 28, 3381.

[30] B. J. Tauro, R. A. Mathias, D. W. Greening, S. K. Gopal, H. Ji, E. A. Kapp, B. M. Coleman, A. F. Hill, U. Kusebauch, J. L. Hallows, D. Shteynberg, R. L. Moritz, H. J. Zhu, R. J. Simpson, Mol. Cell Proteomics 2013, 12, 2148.

[31] G. R. Willis, S. Kourembanas, S. A. Mitsialis, Frontiers in Cardiovascular Medicine 2017, 4, 63.

[32] R. A. Sharples, L. J. Vella, R. M. Nisbet, R. Naylor, K. Perez, K. J. Barnham, C. L. Masters, A. F. Hill, 2008, 22, 1469.

[33] C. Théry, L. Zitvogel, S. Amigorena, Nature Reviews Immunology 2002, 2, 569.

[34] V. J. Yuste, I. Sánchez-López, C. Solé, M. Encinas, J. R. Bayascas, J. Boix, J. X. Comella, 2002, 80, 126.

[35] C. Villarroya-Beltri, F. Baixauli, C. Gutiérrez-Vázquez, F. Sánchez-Madrid, M. Mittelbrunn, Seminars in cancer biology 2014, 28, 3.

[36] S. Keerthikumar, L. Gangoda, M. Liem, P. Fonseka, I. Atukorala, C. Ozcitti, A. Mechler, C. G. Adda, C.-S. Ang, S. Mathivanan, Oncotarget 2015, 6, 15375.

[37] O. Moreno-Gonzalo, I. Fernandez-Delgado, F. Sanchez-Madrid, Cellular and Molecular Life Sciences 2018, 75, 1.

[38] X. Osteikoetxea, A. Balogh, K. Szabó-Taylor, A. Németh, T. G. Szabó, K. Pálóczi, B. Sódar, Á. Kittel, B. György, É. Pállinger, J. Matkó, E. I. Buzás, PLOS ONE 2015, 10, e0121184.

[39] William M. Henne, Nicholas J. Buchkovich, Scott D. Emr, Developmental Cell 2011, 21, 77.

[40] C. Raiborg, H. Stenmark, Nature 2009, 458, 445.

[41] I. Nazarenko, S. Rana, A. Baumann, J. McAlear, A. Hellwig, M. Trendelenburg, G. Lochnit, K. T. Preissner, M. Zoller, Cancer Res 2010, 70, 1668.

[42] S. Rana, M. Zoller, Biochem Soc Trans 2011, 39, 559.

[43] M. Fukuda, E. Kanno, K. Ishibashi, T. Itoh, Molecular & Cellular Proteomics 2008, 7, 1031.

[44] M. T. Lee, A. Mishra, D. G. Lambright, Traffic 2009, 10, 1377.

[45] C. Thery, M. Ostrowski, E. Segura, Nat Rev Immunol 2009, 9, 581.

[46] T. Takata, J. T. Oxford, B. Demeler, K. J. Lampi, Protein Science : A Publication of the Protein Society 2008, 17, 1565.

[47] N. LeBrasseur, The Journal of Cell Biology 2002, 159, 201.

[48] S. Christian, Mass Spectrometry Reviews 2005, 24, 701.

[49] Y. S. Bae, H. Oh, S. G. Rhee, Y. D. Yoo, Molecules and Cells 2011, 32, 491.

[50] T. Geiger, S. Clarke, Journal of Biological Chemistry 1987, 262, 785.

[51] N. E. Robinson, Proceedings of the National Academy of Sciences 2002, 99, 5283.

[52] H. Schulze-Bergkamen, R. Ehrenberg, L. Hickmann, B. Vick, T. Urbanik, C. C. Schimanski, M. R. Berger, A. Schad, A. Weber, S. Heeger, P. R. Galle, M. Moehler, World Journal of Gastroenterology : WJG 2008, 14, 3829.

[53] A. I. Nepomuceno, R. J. Gibson, S. M. Randall, D. C. Muddiman, Journal of proteome research 2014, 13, 777.

[54] D. Ren, G. D. Pipes, D. Liu, L.-Y. Shih, A. C. Nichols, M. J. Treuheit, D. N. Brems, P. V. Bondarenko, Analytical Biochemistry 2009, 392, 12.

[55] J. Landry, H. Lambert, M. Zhou, J. N. Lavoie, E. Hickey, L. A. Weber, C. W. Anderson, Journal of Biological Chemistry 1992, 267, 794.

[56] J. R. Wiśniewski, N. Nagaraj, A. Zougman, F. Gnad, M. Mann, Journal of Proteome Research 2010, 9, 3280.

[57] H. Valadi, K. Ekström, A. Bossios, M. Sjöstrand, J. J. Lee, J. O. Lötvall, Nature Cell Biology 2007, 9, 654.

[58] S. Klein-Scory, M. M. Tehrani, C. Eilert-Micus, K. A. Adamczyk, N. Wojtalewicz, M. Schnölzer, S. A. Hahn, W. Schmiegel, I. Schwarte-Waldhoff, Proteome Science 2014, 12, 50.

[59] S. A. Wagner, P. Beli, B. T. Weinert, M. L. Nielsen, J. Cox, M. Mann, C. Choudhary, Molecular & Cellular Proteomics : MCP 2011, 10, M111.013284.

[60] N. D. Udeshi, P. Mertins, T. Svinkina, S. A. Carr, Nature protocols 2013, 8, 1950.

[61] G. Xu, J. S. Paige, S. R. Jaffrey, Nature biotechnology 2010, 28, 868.

[62] L. Wang, Y. Han, S. Zhou, X. Guan, Biosensors & bioelectronics 2014, 62, 158.

[63] O. Marques, T. F. Outeiro, Cell Death & Disease 2012, 3, e350.

[64] L. Stefanis, Cold Spring Harbor Perspectives in Medicine 2012, 2, a009399.

[65] J.-E. Kim, S. R. Tannenbaum, F. M. White, Journal of Proteome Research 2005, 4, 1339.

[66] A. Castello, B. Fischer, K. Eichelbaum, R. Horos, Benedikt M. Beckmann, C. Strein, Norman E. Davey, David T. Humphreys, T. Preiss, Lars M. Steinmetz, J. Krijgsveld, Matthias W. Hentze, Cell 2012, 149, 1393.

[67] K. Szabó-Taylor, B. Ryan, X. Osteikoetxea, T. G. Szabó, B. Sódar, M. Holub, A. Németh, K. Pálóczi, É. Pállinger, P. Winyard, E. I. Buzás, Seminars in Cell & Developmental Biology 2015, 40, 8.

[68] S. Kreimer, A. M. Belov, I. Ghiran, S. K. Murthy, D. A. Frank, A. R. Ivanov, Journal of Proteome Research 2015, 14, 2367.

[69] C. Xu, O. Nikolova, R. S. Basom, R. M. Mitchell, R. Shaw, R. D. Moser, H. Park, K. E. Gurley, M. C. Kao, C. L. Green, F. X. Schaub, R. L. Diaz, H. A. Swan, I. S. Jang, J. Guinney, V. K. Gadi, A. A. Margolin, C. Grandori, C. J. Kemp, E. Méndez, Clinical Cancer Research 2018, 24, 2828.

[70] R. S. Conlan, S. Pisano, M. I. Oliveira, M. Ferrari, I. Mendes Pinto, Trends in Molecular Medicine 2017, 23, 636.

[71] K. Gilligan, R. Dwyer, International Journal of Molecular Sciences 2017, 18, 1122.

[72] K. T. G. Rigbolt, T. A. Prokhorova, V. Akimov, J. Henningsen, P. T. Johansen, I. Kratchmarova, M. Kassem, M. Mann, J. V. Olsen, B. Blagoev, Science Signaling 2011, 4, rs3.

[73] Z. Guo, L. J. Neilson, H. Zhong, P. S. Murray, M. V. Rao, S. Zanivan, R. Zaidel-Bar, Science signaling 2014, 7, rs7.

[74] A. N. Kettenbach, D. K. Schweppe, B. K. Faherty, D. Pechenick, A. A. Pletnev, S. A. Gerber, Science signaling 2011, 4, 10.1126/scisignal.2001497.

[75] F. Gnad, J. Gunawardena, M. Mann, Nucleic Acids Research 2011, 39, D253.

[76] J. V. Olsen, M. Vermeulen, A. Santamaria, C. Kumar, M. L. Miller, L. J. Jensen, F. Gnad, J. Cox, T. S. Jensen, E. A. Nigg, S. Brunak, M. Mann, Science Signaling 2010, 3, ra3.

[77] P. Mertins, F. Yang, T. Liu, D. R. Mani, V. A. Petyuk, M. A. Gillette, K. R. Clauser, J. W. Qiao, M. A. Gritsenko, R. J. Moore, D. A. Levine, R. Townsend, P. Erdmann-Gilmore, J. E. Snider, S. R. Davies, K. V. Ruggles, D. Fenyo, R. T. Kitchens, S. Li, N. Olvera, F. Dao, H. Rodriguez, D. W. Chan, D. Liebler, F. White, K. D. Rodland, G. B. Mills, R. D. Smith, A. G. Paulovich, M. Ellis, S. A. Carr, Molecular & Cellular Proteomics : MCP 2014, 13, 1690.

[78] A. Santamaria, B. Wang, S. Elowe, R. Malik, F. Zhang, M. Bauer, A. Schmidt, H. H. W. Silljé, R. Körner, E. A. Nigg, Molecular & Cellular Proteomics : MCP 2011, 10, M110.004457.

FIGURE LEGENDS

Figure 1. Schematic diagram representing the work flow used to generate and isolate M-NVs and exosomes

(A) Experimental workflow used to generate and isolate M-NVs and exosomes (Exos). SH-SY5Y (1.2×10^8) cells were resuspended in DPBS and serially extruded through 10, 5 and 1 μm membranes by an Avanti-mini extruder. The extruded cell-derived vesicles were loaded on to an OptiPrep™ gradient and centrifuged at 100,000 g for 2 h. Subsequently, F6 was collected and considered as M-NVs following characterization. (B) The conditioned media was collected from each flask and centrifuged at 2000 g for 10 min to remove cell debris. The supernatant centrifuged at 10,000 g for 30 min at 4° C to remove microvesicles. The resultant supernatant was centrifuged at 100,000 g for 70 min at 4° C to pellet Exos. Washing step was carried out by resuspending Exos with DPBS and centrifuged at 100,000 g for 70 min at 4° C.

Figure 2. Biophysical characterization of exosomes and M-NVs

(A) Nanoparticle tracking analysis of Exos and M-NVs highlight size (diameter) distribution and a mode of 179 nm for Exos and 186 nm for M-NVs (N=4). (B) Transmission electron microscopy reveal Exos and M-NVs with intact lipid bilayer. Scale bar, 500 nm. (C) M-NVs and Exos particle counts and protein concentration was normalized to total cell number (N=4).

Figure 3. Proteomic profiling of cells, exosomes and M-NVs

(A) Silver staining of cells, Exos and M-NVs reveal similar and distinct protein profile differences. (B) Western blot analysis of exosomal and non exosomal proteins. (C) Discovery-based proteomic profiling, analysed by nLC-MS/MS, was performed for M-NVs, Exos and parental cells. Venn diagram showing the number of proteins identified with FDR of 1% (protein/peptide level) (N=4, N=2); a total of 4,269 proteins were identified in all sample types, with 1,887 common (~44% of all identified proteins) and 19 and 65 proteins uniquely identified in M-NVs and Exos, respectively. (D) Principal component analysis of global proteome for each individual biological and technical replicate for each sample set, highlighting similarity in M-NVs and parental cell profiles, as distinct from Exos.

Figure 4. M-NVs contain distinct proteome to exosomes

(A) Hierarchical clustering of protein expression between M-NVs and Exos. (B) Volcano plot showing quantitative difference of protein expression between M-NVs and Exos using adjusted p-value>0.05 (-log10 = 1.3) and a 2-fold difference (log2=±1). (C) Gene ontology (GO) enrichment annotation based on molecular function and biological process between M-NVs and Exos.

Figure 5. Heat map of proteins within GO associated functions in exosomes and M-NVs

Heat map of significantly enriched and shared (commonly expressed) proteins from quantitative mass spectrometry analysis of Exos and M-NVs, based on Z-scored label-free quantification (LFQ) values (biological N=4 replicates). These enriched protein subsets were correlated with GO enrichment annotation based on molecular function and biological process between M-NVs and Exos. The percentage of proteins that are represented in each set of GO functions are indicated between Exos versus M-NVs.

Figure 6. Distinct protein PTMs profiles in M-NVs compared to exosomes

(A) Informatic workflow used for global identification of PTMs from M-NVs and Exos. Data was searched using PEAKS and MaxQuant for protein and PTM identifications against 11 known protein modifications as variable modifications. (B) Hierarchical clustering analysis, indicating similarity and variance between protein PTM abundance in M-NVs and Exos. (C) Z-score normalized ratio profile and distribution visualization of enriched PTMs using adjusted p-value>0.05 (-log10 = 1.3) and a 2-fold difference (log2=±1).

SUPPLEMENTARY DATA

Supplementary Figure S1

M-NVs purification using OptiPrep™ density gradient separation. SH-SY5Y (1.2×10^8 cells) were resuspended in DPBS and serially extruded through 10, 5 and 1 μm membranes by an Avanti-mini extruder. The extruded cell-derived vesicles were loaded on to an OptiPrep™ gradient and centrifuged at 100,000 g for 2 h. Subsequently, all fractions (F1-F7) were isolated and 40 μL for each fraction separated by SDS-PAGE and stained with Coomassie Blue. F6 was considered as mimetic-NVs.

Supplementary Table 1.

Overview of proteins identified in M-NVs, Exos, and parental cells including the unique proteins identified in M-NVs, Exos and cells, respectively.

Supplementary Table 2.

Overview of the PTMs found significantly regulated in M-NV compared to the Exos. The regulation is shown in log2. p-value, which correspond to the adjusted p-value from student's t-test using the Benjamini-Hochberg post-doc procedure. *p<0.05, **p<01, (-) not calculated. MaxQ = Found by MaxQuant (and PEAKS) NF = Not found by MaxQuant, NS = Not searched in MaxQuant. Numbers are literature references: [59, 65, 72-78] shown in cases with dimethylation and triphosphorylations, where methylation or phosphorylation is found in literature on site respectively.

Supplementary Table 3.

Overview of the PTMs regulation on proteins found enriched in M-NV. The regulation is shown in log2. p-value, which correspond to the adjusted p-value from student's t-test using the Benjamini-Hochberg post-doc procedure. *p<0.05, **p<01, (-) not calculated.

Supplementary Table 4.

Overview of the PTMs regulation on proteins found enriched in Exos. The regulation is shown in log2. p-value, which correspond to the adjusted p-value from student's t-test using the Benjamini-Hochberg post-doc procedure. *p<0.05, **p<01, (-) not calculated.

Table 1. Enriched top 100 in M-NVs

Protein Accession	Entry name	Gene	Protein names
P42166	LAP2A_HUMAN	TMPO	Lamina-associated polypeptide 2, isoform alpha (Thymopoietin isoform alpha) (TP alpha) (Thymopoietin-related peptide isoform alpha) (TPRP isoform alpha) [Cleaved into: Thymopoietin (TP) (Splenin); Thymopentin (TP5)]
P42167	LAP2B_HUMAN	TMPO	Lamina-associated polypeptide 2, isoforms beta/gamma (Thymopoietin, isoforms beta/gamma) (TP beta/gamma) (Thymopoietin-related peptide isoforms beta/gamma) (TPRP isoforms beta/gamma) [Cleaved into: Thymopoietin (TP) (Splenin); Thymopentin (TP5)]
P38159	RBMX_HUMAN	RBMX	RNA-binding motif protein, X chromosome (Glycoprotein p43) (Heterogeneous nuclear ribonucleoprotein G) (hnRNP G) [Cleaved into: RNA-binding motif protein, X chromosome, N-terminally processed]
Q9Y6C9	MTCH2_HUMAN	MTCH2	Mitochondrial carrier homolog 2 (Met-induced mitochondrial protein)
Q9NS69	TOM22_HUMAN	TOMM22	Mitochondrial import receptor subunit TOM22 homolog (hTom22) (1C9-2) (Translocase of outer membrane 22 kDa subunit homolog)
P28331	NDUS1_HUMAN	NDUFS1	NADH-ubiquinone oxidoreductase 75 kDa subunit, mitochondrial (EC 1.6.5.3) (EC 1.6.99.3) (Complex I-75kD) (CI-75kD)
Q13423	NNTM_HUMAN	NNT	NAD(P) transhydrogenase, mitochondrial (EC 1.6.1.2) (Nicotinamide nucleotide transhydrogenase) (Pyridine nucleotide transhydrogenase)
P22695	QCR2_HUMAN	UQCRC2	Cytochrome b-c1 complex subunit 2, mitochondrial (Complex III subunit 2) (Core protein II) (Ubiquinol-cytochrome-c reductase complex core protein 2)
Q6NUK1	SCMC1_HUMAN	SLC25A24	Calcium-binding mitochondrial carrier protein SCaMC-1 (Mitochondrial ATP-Mg/Pi carrier protein 1) (Mitochondrial Ca(2+)-dependent solute carrier protein 1) (Small calcium-binding mitochondrial carrier protein 1) (Solute carrier family 25 member 24)
P20674	COX5A_HUMAN	COX5A	Cytochrome c oxidase subunit 5A, mitochondrial (Cytochrome c oxidase polypeptide Va)
O95202	LETM1_HUMAN	LETM1	Mitochondrial proton/calcium exchanger protein (Leucine zipper-EF-hand-containing transmembrane protein 1)
Q9BWM7	SFXN3_HUMAN	SFXN3	Sideroflexin-3

P14854	CX6B1_HUMAN	COX6B1	Cytochrome c oxidase subunit 6B1 (Cytochrome c oxidase subunit VIb isoform 1) (COX VIb-1)
Q8IXI1	MIRO2_HUMAN	RHOT2	Mitochondrial Rho GTPase 2 (MIRO-2) (hMiro-2) (EC 3.6.5.-) (Ras homolog gene family member T2)
O75306	NDUS2_HUMAN	NDUFS2	NADH dehydrogenase [ubiquinone] iron-sulfur protein 2, mitochondrial (EC 1.6.5.3) (EC 1.6.99.3) (Complex I-49kD) (CI-49kD) (NADH-ubiquinone oxidoreductase 49 kDa subunit)
P12235	ADT1_HUMAN	SLC25A4	ADP/ATP translocase 1 (ADP,ATP carrier protein 1) (ADP,ATP carrier protein, heart/skeletal muscle isoform T1) (Adenine nucleotide translocator 1) (ANT 1) (Solute carrier family 25 member 4)
O94826	TOM70_HUMAN	TOMM70	Mitochondrial import receptor subunit TOM70 (Mitochondrial precursor proteins import receptor) (Translocase of outer membrane 70 kDa subunit) (Translocase of outer mitochondrial membrane protein 70)
Q9NVI7	ATD3A_HUMAN	ATAD3A	ATPase family AAA domain-containing protein 3A
Q9UJS0	CMC2_HUMAN	SLC25A13	Calcium-binding mitochondrial carrier protein Aralar2 (Citrin) (Mitochondrial aspartate glutamate carrier 2) (Solute carrier family 25 member 13)
Q8TEM1	PO210_HUMAN	NUP210	Nuclear pore membrane glycoprotein 210 (Nuclear pore protein gp210) (Nuclear envelope pore membrane protein POM 210) (POM210) (Nucleoporin Nup210) (Pore membrane protein of 210 kDa)
Q15287	RNPS1_HUMAN	RNPS1	RNA-binding protein with serine-rich domain 1 (SR-related protein LDC2)
Q9Y4W6	AFG32_HUMAN	AFG3L2	AFG3-like protein 2 (EC 3.4.24.-) (Paraplegin-like protein)
P31930	QCR1_HUMAN	UQCRC1	Cytochrome b-c1 complex subunit 1, mitochondrial (Complex III subunit 1) (Core protein I) (Ubiquinol-cytochrome-c reductase complex core protein 1)
Q3ZCQ8	TIM50_HUMAN	TIMM50	Mitochondrial import inner membrane translocase subunit TIM50
Q86UP2	KTN1_HUMAN	KTN1	Kinectin (CG-1 antigen) (Kinesin receptor)
Q99459	CDC5L_HUMAN	CDC5L	Cell division cycle 5-like protein (Cdc5-like protein) (Pombe cdc5-related protein)
Q9Y512	SAM50_HUMAN	SAMM50	Sorting and assembly machinery component 50 homolog (Transformation-related gene 3 protein) (TRG-3)
Q96HS1	PGAM5_HUMAN	PGAM5	Serine/threonine-protein phosphatase PGAM5, mitochondrial (EC 3.1.3.16) (Bcl-XL-binding protein v68) (Phosphoglycerate mutase family member 5)
Q53H12	AGK_HUMAN	AGK	Acylglycerol kinase, mitochondrial (hAGK) (EC 2.7.1.107) (EC 2.7.1.94) (Multiple substrate lipid kinase) (HsMuLK) (MuLK) (Multi-substrate lipid kinase)
Q9P0J0	NDUAD_HUMAN	NDUFA13	NADH dehydrogenase [ubiquinone] 1 alpha subcomplex subunit 13 (Cell death regulatory protein GRIM-19) (Complex I-B16.6) (CI-B16.6) (Gene associated with retinoic and interferon-induced mortality 19 protein) (GRIM-19) (Gene associated with retinoic and IFN-induced mortality 19 protein) (NADH-ubiquinone oxidoreductase B16.6 subunit)
Q8IY81	SPB1_HUMAN	FTSJ3	pre-rRNA processing protein FTSJ3 (EC 2.1.1.-) (2'-O-ribose RNA methyltransferase SPB1 homolog) (Protein ftsJ homolog 3) (Putative rRNA methyltransferase 3)
Q02978	M2OM_HUMAN	SLC25A11	Mitochondrial 2-oxoglutarate/malate carrier protein (OGCP) (Solute carrier family 25 member 11)
O95831	AIFM1_HUMAN	AIFM1	Apoptosis-inducing factor 1, mitochondrial (EC 1.1.1.-) (Programmed cell death protein 8)
P00167	CYB5_HUMAN	CYB5A	Cytochrome b5 (Microsomal cytochrome b5 type A) (MCB5)
O75947	ATP5H_HUMAN	ATP5H	ATP synthase subunit d, mitochondrial (ATPase subunit d)

Q12906	ILF3_HUMAN	ILF3	Interleukin enhancer-binding factor 3 (Double-stranded RNA-binding protein 76) (DRBP76) (M-phase phosphoprotein 4) (MPP4) (Nuclear factor associated with dsRNA) (NFAR) (Nuclear factor of activated T-cells 90 kDa) (NF-AT-90) (Translational control protein 80) (TCP80)
O00217	NDUS8_HUMAN	NDUFS8	NADH dehydrogenase [ubiquinone] iron-sulfur protein 8, mitochondrial (EC 1.6.5.3) (EC 1.6.99.3) (Complex I-23kD) (CI-23kD) (NADH-ubiquinone oxidoreductase 23 kDa subunit) (TYKY subunit)
P18859	ATP5J_HUMAN	ATP5J	ATP synthase-coupling factor 6, mitochondrial (ATPase subunit F6)
P08574	CY1_HUMAN	CYC1	Cytochrome c1, heme protein, mitochondrial (Complex III subunit 4) (Complex III subunit IV) (Cytochrome b-c1 complex subunit 4) (Ubiquinol-cytochrome-c reductase complex cytochrome c1 subunit) (Cytochrome c-1)
P49821	NDUV1_HUMAN	NDUFV1	NADH dehydrogenase [ubiquinone] flavoprotein 1, mitochondrial (EC 1.6.5.3) (EC 1.6.99.3) (Complex I-51kD) (CI-51kD) (NADH dehydrogenase flavoprotein 1) (NADH-ubiquinone oxidoreductase 51 kDa subunit)
P43304	GPDM_HUMAN	GPD2	Glycerol-3-phosphate dehydrogenase, mitochondrial (GPD-M) (GPDH-M) (EC 1.1.5.3) (mtGPD)
P56385	ATP5I_HUMAN	ATP5I	ATP synthase subunit e, mitochondrial (ATPase subunit e) [Cleaved into: ATP synthase subunit e, mitochondrial, N-terminally processed]
Q9NVH1	DJC11_HUMAN	DNAJC11	DnaJ homolog subfamily C member 11
Q969V3	NCLN_HUMAN	NCLN	Nicalin (Nicastrin-like protein)
P50416	CPT1A_HUMAN	CPT1A	Carnitine O-palmitoyltransferase 1, liver isoform (CPT1-L) (EC 2.3.1.21) (Carnitine O-palmitoyltransferase I, liver isoform) (CPT I) (CPTI-L) (Carnitine palmitoyltransferase 1A)
Q14690	RRP5_HUMAN	PDCD11	Protein RRP5 homolog (NF-kappa-B-binding protein) (NFBP) (Programmed cell death protein 11)
Q14739	LBR_HUMAN	LBR	Lamin-B receptor (Integral nuclear envelope inner membrane protein) (LMN2R)
Q16795	NDUA9_HUMAN	NDUFA9	NADH dehydrogenase [ubiquinone] 1 alpha subcomplex subunit 9, mitochondrial (Complex I-39kD) (CI-39kD) (NADH-ubiquinone oxidoreductase 39 kDa subunit)
O95793	STAU1_HUMAN	STAU1	Double-stranded RNA-binding protein Staufen homolog 1
P52815	RM12_HUMAN	MRPL12	39S ribosomal protein L12, mitochondrial (L12mt) (MRP-L12) (5c5-2) (Mitochondrial large ribosomal subunit protein bL12m)
O94905	ERLN2_HUMAN	ERLIN2	Erlin-2 (Endoplasmic reticulum lipid raft-associated protein 2) (Stomatin-prohibitin-flotillin-HflC/K domain-containing protein 2) (SPFH domain-containing protein 2)
Q13435	SF3B2_HUMAN	SF3B2	Splicing factor 3B subunit 2 (Pre-mRNA-splicing factor SF3b 145 kDa subunit) (SF3b145) (Spliceosome-associated protein 145) (SAP 145)
Q53GS9	SNUT2_HUMAN	USP39	U4/U6.U5 tri-snRNP-associated protein 2 (Inactive ubiquitin-specific peptidase 39) (SAD1 homolog) (U4/U6.U5 tri-snRNP-associated 65 kDa protein) (65K)
O00483	NDUA4_HUMAN	NDUFA4	Cytochrome c oxidase subunit NDUFA4 (Complex I-MLRQ) (CI-MLRQ) (NADH-ubiquinone oxidoreductase MLRQ subunit)
P19404	NDUV2_HUMAN	NDUFV2	NADH dehydrogenase [ubiquinone] flavoprotein 2, mitochondrial (EC 1.6.5.3) (EC 1.6.99.3) (NADH-ubiquinone oxidoreductase 24 kDa subunit)
Q9H3N1	TMX1_HUMAN	TMX1	Thioredoxin-related transmembrane protein 1 (Thioredoxin domain-containing protein 1) (Transmembrane Trx-related protein)
P18583	SON_HUMAN	SON	Protein SON (Bax antagonist selected in saccharomyces 1) (BASS1) (Negative regulatory element-binding protein) (NRE-binding protein) (Protein DBP-5) (SON3)

Q8NBX0	SCPDL_HUMAN	SCCPDH	Saccharopine dehydrogenase-like oxidoreductase (EC 1.-.-.-)
P13073	COX41_HUMAN	COX4I1	Cytochrome c oxidase subunit 4 isoform 1, mitochondrial (Cytochrome c oxidase polypeptide IV) (Cytochrome c oxidase subunit IV isoform 1) (COX IV-1)
Q96CS3	FAF2_HUMAN	FAF2	FAS-associated factor 2 (Protein ETEA) (UBX domain-containing protein 3B) (UBX domain-containing protein 8)
P21912	SDHB_HUMAN	SDHB	Succinate dehydrogenase [ubiquinone] iron-sulfur subunit, mitochondrial (EC 1.3.5.1) (Iron-sulfur subunit of complex II) (Ip)
O95864	FADS2_HUMAN	FADS2	Fatty acid desaturase 2 (EC 1.14.19.3) (Acyl-CoA 6-desaturase) (Delta(6) fatty acid desaturase) (D6D) (Delta(6) desaturase) (Delta-6 desaturase)
Q16718	NDUA5_HUMAN	NDUFA5	NADH dehydrogenase [ubiquinone] 1 alpha subcomplex subunit 5 (Complex I subunit B13) (Complex I-13kD-B) (CI-13kD-B) (NADH-ubiquinone oxidoreductase 13 kDa-B subunit)
O96000	NDUBA_HUMAN	NDUFB10	NADH dehydrogenase [ubiquinone] 1 beta subcomplex subunit 10 (Complex I-PDSW) (CI-PDSW) (NADH-ubiquinone oxidoreductase PDSW subunit)
Q15424	SAFB1_HUMAN	SAFB	Scaffold attachment factor B1 (SAF-B) (SAF-B1) (HSP27 estrogen response element-TATA box-binding protein) (HSP27 ERE-TATA-binding protein)
Q9H9B4	SFXN1_HUMAN	SFXN1	Sideroflexin-1 (Tricarboxylate carrier protein) (TCC)
Q9Y6M9	NDUB9_HUMAN	NDUFB9	NADH dehydrogenase [ubiquinone] 1 beta subcomplex subunit 9 (Complex I-B22) (CI-B22) (LYR motif-containing protein 3) (NADH-ubiquinone oxidoreductase B22 subunit)
P46087	NOP2_HUMAN	NOP2	Probable 28S rRNA (cytosine(4447)-C(5))-methyltransferase (EC 2.1.1.-) (Nucleolar protein 1) (Nucleolar protein 2 homolog) (Proliferating-cell nucleolar antigen p120) (Proliferation-associated nucleolar protein p120)
P10515	ODP2_HUMAN	DLAT	Dihydrolipoyllysine-residue acetyltransferase component of pyruvate dehydrogenase complex, mitochondrial (EC 2.3.1.12) (70 kDa mitochondrial autoantigen of primary biliary cirrhosis) (PBC) (Dihydrolipoamide acetyltransferase component of pyruvate dehydrogenase complex) (M2 antigen complex 70 kDa subunit) (Pyruvate dehydrogenase complex component E2) (PDC-E2) (PDCE2)
Q8TCJ2	STT3B_HUMAN	STT3B	Dolichyl-diphosphooligosaccharide--protein glycosyltransferase subunit STT3B (Oligosaccharyl transferase subunit STT3B) (STT3-B) (EC 2.4.99.18) (Source of immunodominant MHC-associated peptides homolog)
Q96PK6	RBM14_HUMAN	RBM14	RNA-binding protein 14 (Paraspeckle protein 2) (PSP2) (RNA-binding motif protein 14) (RRM-containing coactivator activator/modulator) (Synaptotagmin-interacting protein) (SYT-interacting protein)
P36542	ATPG_HUMAN	ATP5F1C	ATP synthase subunit gamma, mitochondrial (ATP synthase F1 subunit gamma) (F-ATPase gamma subunit)
P55084	ECHB_HUMAN	HADHB	Trifunctional enzyme subunit beta, mitochondrial (TP-beta) [Includes: 3-ketoacyl-CoA thiolase (EC 2.3.1.16) (Acetyl-CoA acyltransferase) (Beta-ketothiolase)]
Q96A33	CCD47_HUMAN	CCDC47	Coiled-coil domain-containing protein 47
Q03701	CEBPZ_HUMAN	CEBPZ	CCAAT/enhancer-binding protein zeta (CCAAT-box-binding transcription factor) (CBF) (CCAAT-binding factor)
P10606	COX5B_HUMAN	COX5B	Cytochrome c oxidase subunit 5B, mitochondrial (Cytochrome c oxidase polypeptide Vb)
Q86UE4	LYRIC_HUMAN	MTDH	Protein LYRIC (3D3/LYRIC) (Astrocyte elevated gene-1 protein) (AEG-1) (Lysine-rich CEACAM1 co-isolated protein) (Metadherin) (Metastasis adhesion protein)

Q8NEJ9	NGDN_HUMAN	NGDN	Neuroguidin (Centromere accumulated nuclear protein 1) (CANu1) (EIF4E-binding protein)
Q8TB36	GDAP1_HUMAN	GDAP1	Ganglioside-induced differentiation-associated protein 1 (GDAP1)
Q9UHA4	LTOR3_HUMAN	LAMTOR3	Ragulator complex protein LAMTOR3 (Late endosomal/lysosomal adaptor and MAPK and MTOR activator 3) (MEK-binding partner 1) (Mp1) (Mitogen-activated protein kinase kinase 1-interacting protein 1) (Mitogen-activated protein kinase scaffold protein 1)
Q9UBX3	DIC_HUMAN	SLC25A10	Mitochondrial dicarboxylate carrier (Solute carrier family 25 member 10)
P31040	SDHA_HUMAN	SDHA	Succinate dehydrogenase [ubiquinone] flavoprotein subunit, mitochondrial (EC 1.3.5.1) (Flavoprotein subunit of complex II) (Fp)
Q03252	LMNB2_HUMAN	LMNB2	Lamin-B2
P07919	QCR6_HUMAN	UQCRH	Cytochrome b-c1 complex subunit 6, mitochondrial (Complex III subunit 6) (Complex III subunit VIII) (Cytochrome c1 non-heme 11 kDa protein) (Mitochondrial hinge protein) (Ubiquinol-cytochrome c reductase complex 11 kDa protein)
P28288	ABCD3_HUMAN	ABCD3	ATP-binding cassette sub-family D member 3 (70 kDa peroxisomal membrane protein) (PMP70)
Q96AG4	LRC59_HUMAN	LRRC59	Leucine-rich repeat-containing protein 59 (Ribosome-binding protein p34) (p34) [Cleaved into: Leucine-rich repeat-containing protein 59, N-terminally processed]
P55265	DSRAD_HUMAN	ADAR	Double-stranded RNA-specific adenosine deaminase (DRADA) (EC 3.5.4.37) (136 kDa double-stranded RNA-binding protein) (p136) (Interferon-inducible protein 4) (IFI-4) (K88DSRBP)
Q9NW13	RBM28_HUMAN	RBM28	RNA-binding protein 28 (RNA-binding motif protein 28)
P56134	ATPK_HUMAN	ATP5J2	ATP synthase subunit f, mitochondrial
O75489	NDUS3_HUMAN	NDUFS3	NADH dehydrogenase [ubiquinone] iron-sulfur protein 3, mitochondrial (EC 1.6.5.3) (EC 1.6.99.3) (Complex I-30kD) (CI-30kD) (NADH-ubiquinone oxidoreductase 30 kDa subunit)
O14967	CLGN_HUMAN	CLGN	Calmegin
O95299	NDUAA_HUMAN	NDUFA10	NADH dehydrogenase [ubiquinone] 1 alpha subcomplex subunit 10, mitochondrial (Complex I-42kD) (CI-42kD) (NADH-ubiquinone oxidoreductase 42 kDa subunit)
Q9Y2W1	TR150_HUMAN	THRAP3	Thyroid hormone receptor-associated protein 3 (BCLAF1 and THRAP3 family member 2) (Thyroid hormone receptor-associated protein complex 150 kDa component) (Trap150)
Q9P2K5	MYEF2_HUMAN	MYEF2	Myelin expression factor 2 (MEF-2) (MyEF-2) (MST156)
Q9UGP8	SEC63_HUMAN	SEC63	Translocation protein SEC63 homolog
P57105	SYJ2B_HUMAN	SYNJ2BP	Synaptojanin-2-binding protein (Mitochondrial outer membrane protein 25)
P49458	SRP09_HUMAN	SRP9	Signal recognition particle 9 kDa protein (SRP9)
Q5JPE7	NOMO2_HUMAN	NOMO2	Nodal modulator 2 (pM5 protein 2)
Q00765	REEP5_HUMAN	REEP5	Receptor expression-enhancing protein 5 (Polyposis locus protein 1) (Protein TB2)
P19338	NUCL_HUMAN	NCL	Nucleolin (Protein C23)

Table 2. Cell surface, plasma membrane and associated

Protein	Entry name	Protein names	Gene

Accession			
Q12797	ASPH_HUMAN	Aspartyl/asparaginyl beta-hydroxylase (EC 1.14.11.16) (Aspartate beta-hydroxylase) (ASP beta-hydroxylase) (Peptide-aspartate beta-dioxygenase)	ASPH
P01891	1A68_HUMAN	HLA class I histocompatibility antigen, A-68 alpha chain (Aw-68) (HLA class I histocompatibility antigen, A-28 alpha chain) (MHC class I antigen A*68)	HLA-A
P01892	1A02_HUMAN	HLA class I histocompatibility antigen, A-2 alpha chain (MHC class I antigen A*2)	HLA-A
P04439	1A03_HUMAN	HLA class I histocompatibility antigen, A-3 alpha chain (MHC class I antigen A*3)	HLA-A
P05534	1A24_HUMAN	HLA class I histocompatibility antigen, A-24 alpha chain (Aw-24) (HLA class I histocompatibility antigen, A-9 alpha chain) (MHC class I antigen A*24)	HLA-A
P10314	1A32_HUMAN	HLA class I histocompatibility antigen, A-32 alpha chain (MHC class I antigen A*32)	HLA-A
P10316	1A69_HUMAN	HLA class I histocompatibility antigen, A-69 alpha chain (Aw-69) (HLA class I histocompatibility antigen, A-28 alpha chain) (MHC class I antigen A*69)	HLA-A
P13746	1A11_HUMAN	HLA class I histocompatibility antigen, A-11 alpha chain (MHC class I antigen A*11)	HLA-A
P16188	1A30_HUMAN	HLA class I histocompatibility antigen, A-30 alpha chain (MHC class I antigen A*30)	HLA-A
P16189	1A31_HUMAN	HLA class I histocompatibility antigen, A-31 alpha chain (MHC class I antigen A*31)	HLA-A
P16190	1A33_HUMAN	HLA class I histocompatibility antigen, A-33 alpha chain (Aw-19) (Aw-33) (MHC class I antigen A*33)	HLA-A
P18462	1A25_HUMAN	HLA class I histocompatibility antigen, A-25 alpha chain (HLA class I histocompatibility antigen, A-10 alpha chain) (MHC class I antigen A*25)	HLA-A
P30443	1A01_HUMAN	HLA class I histocompatibility antigen, A-1 alpha chain (MHC class I antigen A*1)	HLA-A
P30447	1A23_HUMAN	HLA class I histocompatibility antigen, A-23 alpha chain (HLA class I histocompatibility antigen, A-9 alpha chain) (MHC class I antigen A*23)	HLA-A
P30450	1A26_HUMAN	HLA class I histocompatibility antigen, A-26 alpha chain (MHC class I antigen A*26)	HLA-A
P30453	1A34_HUMAN	HLA class I histocompatibility antigen, A-34 alpha chain (Aw-34) (HLA class I histocompatibility antigen, A-10 alpha chain) (MHC class I antigen A*34)	HLA-A
P30455	1A36_HUMAN	HLA class I histocompatibility antigen, A-36 alpha chain (Aw-36) (MHC class I antigen A*36)	HLA-A
P30456	1A43_HUMAN	HLA class I histocompatibility antigen, A-43 alpha chain (Aw-43) (MHC class I antigen A*43)	HLA-A
P30457	1A66_HUMAN	HLA class I histocompatibility antigen, A-66 alpha chain (Aw-66) (HLA class I histocompatibility antigen, A-10 alpha chain) (MHC class I antigen A*66)	HLA-A
P30459	1A74_HUMAN	HLA class I histocompatibility antigen, A-74 alpha chain (Aw-19) (Aw-74) (MHC class I antigen A*74)	HLA-A
P30512	1A29_HUMAN	HLA class I histocompatibility antigen, A-29 alpha chain (Aw-19) (MHC class I antigen A*29)	HLA-A
Q09160	1A80_HUMAN	HLA class I histocompatibility antigen, A-80 alpha chain (Aw-80) (HLA class I histocompatibility antigen, A-1 alpha chain) (MHC class I antigen A*80)	HLA-A
Q14696	MESD_HUMAN	LRP chaperone MESD (LDLR chaperone MESD) (Mesoderm development LRP chaperone MESD) (Mesoderm development candidate 2) (Mesoderm development protein) (Renal carcinoma antigen NY-REN-61)	MESD
Q6P1M0	S27A4_HUMAN	Long-chain fatty acid transport protein 4 (FATP-4) (Fatty acid transport protein 4) (EC 6.2.1.-)	SLC27A4

		(Solute carrier family 27 member 4)	
Q9Y2Q0	AT8A1_HUMAN	Phospholipid-transporting ATPase IA (EC 3.6.3.1) (ATPase class I type 8A member 1) (Chromaffin granule ATPase II) (P4-ATPase flippase complex alpha subunit ATP8A1)	ATP8A1
Q86YS7	C2CD5_HUMAN	C2 domain-containing protein 5 (C2 domain-containing phosphoprotein of 138 kDa)	C2CD5
Q8ND76	CCNY_HUMAN	Cyclin-Y (Cyc-Y) (Cyclin box protein 1) (Cyclin fold protein 1) (cyclin-X)	CCNY
P10909	CLUS_HUMAN	Clusterin (Aging-associated gene 4 protein) (Apolipoprotein J) (Apo-J) (Complement cytolysis inhibitor) (CLI) (Complement-associated protein SP-40,40) (Ku70-binding protein 1) (NA1/NA2) (Testosterone-repressed prostate message 2) (TRPM-2) [Cleaved into: Clusterin beta chain (ApoJalpha) (Complement cytolysis inhibitor a chain); Clusterin alpha chain (ApoJbeta) (Complement cytolysis inhibitor b chain)]	CLU
Q8N144	CXD3_HUMAN	Gap junction delta-3 protein (Connexin-31.9) (Cx31.9) (Gap junction alpha-11 protein) (Gap junction chi-1 protein)	GJD3
P54652	HSP72_HUMAN	Heat shock-related 70 kDa protein 2 (Heat shock 70 kDa protein 2)	HSPA2
P23229	ITA6_HUMAN	Integrin alpha-6 (CD49 antigen-like family member F) (VLA-6) (CD antigen CD49f) [Cleaved into: Integrin alpha-6 heavy chain; Integrin alpha-6 light chain; Processed integrin alpha-6 (Alpha6p)]	ITGA6
P08582	TRFM_HUMAN	Melanotransferrin (Melanoma-associated antigen p97) (CD antigen CD228)	MELTF
Q99755	PI51A_HUMAN	Phosphatidylinositol 4-phosphate 5-kinase type-1 alpha (PIP5K1-alpha) (PtdIns(4)P-5-kinase 1 alpha) (EC 2.7.1.68) (68 kDa type I phosphatidylinositol 4-phosphate 5-kinase alpha) (Phosphatidylinositol 4-phosphate 5-kinase type I alpha) (PIP5KIalpha)	PIP5K1A
Q9H0T7	RAB17_HUMAN	Ras-related protein Rab-17	RAB17
P08183	MDR1_HUMAN	Multidrug resistance protein 1 (EC 3.6.3.44) (ATP-binding cassette sub-family B member 1) (P-glycoprotein 1) (CD antigen CD243)	ABCB1
O14672	ADA10_HUMAN	Disintegrin and metalloproteinase domain-containing protein 10 (ADAM 10) (EC 3.4.24.81) (CDw156) (Kuzbanian protein homolog) (Mammalian disintegrin-metalloprotease) (CD antigen CD156c)	ADAM10
P78536	ADA17_HUMAN	Disintegrin and metalloproteinase domain-containing protein 17 (ADAM 17) (EC 3.4.24.86) (Snake venom-like protease) (TNF-alpha convertase) (TNF-alpha-converting enzyme) (CD antigen CD156b)	ADAM17
Q12904	AIMP1_HUMAN	Aminoacyl tRNA synthase complex-interacting multifunctional protein 1 (Multisynthase complex auxiliary component p43) [Cleaved into: Endothelial monocyte-activating polypeptide 2 (EMAP-2) (Endothelial monocyte-activating polypeptide II) (EMAP-II) (Small inducible cytokine subfamily E member 1)]	AIMP1
Q4KMQ2	ANO6_HUMAN	Anoctamin-6 (Small-conductance calcium-activated nonselective cation channel) (SCAN channel) (Transmembrane protein 16F)	ANO6
P07355	ANXA2_HUMAN	Annexin A2 (Annexin II) (Annexin-2) (Calpactin I heavy chain) (Calpactin-1 heavy chain) (Chromobindin-8) (Lipocortin II) (Placental anticoagulant protein IV) (PAP-IV) (Protein I) (p36)	ANXA2
Q9HDC9	APMAP_HUMAN	Adipocyte plasma membrane-associated protein (Protein BSCv)	APMAP
P05023	AT1A1_HUMAN	Sodium/potassium-transporting ATPase subunit alpha-1 (Na(+)/K(+) ATPase alpha-1 subunit) (EC 3.6.3.9) (Sodium pump subunit alpha-1)	ATP1A1
P13637	AT1A3_HUMAN	Sodium/potassium-transporting ATPase subunit alpha-3 (Na(+)/K(+) ATPase alpha-3 subunit) (EC 3.6.3.9) (Na(+)/K(+) ATPase alpha(III) subunit) (Sodium pump subunit alpha-3)	ATP1A3
P05026	AT1B1_HUMAN	Sodium/potassium-transporting ATPase subunit beta-1 (Sodium/potassium-dependent ATPase	ATP1B1

		subunit beta-1)	
P54709	AT1B3_HUMAN	Sodium/potassium-transporting ATPase subunit beta-3 (Sodium/potassium-dependent ATPase subunit beta-3) (ATPB-3) (CD antigen CD298)	ATP1B3
P06576	ATPB_HUMAN	ATP synthase subunit beta, mitochondrial (EC 3.6.3.14) (ATP synthase F1 subunit beta)	ATP5F1B
Q04656	ATP7A_HUMAN	Copper-transporting ATPase 1 (EC 3.6.3.54) (Copper pump 1) (Menkes disease-associated protein)	ATP7A
P35613	BASI_HUMAN	Basigin (5F7) (Collagenase stimulatory factor) (Extracellular matrix metalloproteinase inducer) (EMMPRIN) (Leukocyte activation antigen M6) (OK blood group antigen) (Tumor cell-derived collagenase stimulatory factor) (TCSF) (CD antigen CD147)	BSG
Q07021	C1QBP_HUMAN	Complement component 1 Q subcomponent-binding protein, mitochondrial (ASF/SF2-associated protein p32) (Glycoprotein gC1qBP) (C1qBP) (Hyaluronan-binding protein 1) (Mitochondrial matrix protein p32) (gC1q-R protein) (p33)	C1QBP
P27797	CALR_HUMAN	Calreticulin (CRP55) (Calregulin) (Endoplasmic reticulum resident protein 60) (ERp60) (HACBP) (grp60)	CALR
O15484	CAN5_HUMAN	Calpain-5 (EC 3.4.22.-) (Calpain htra-3) (New calpain 3) (nCL-3)	CAPN5
P48509	CD151_HUMAN	CD151 antigen (GP27) (Membrane glycoprotein SFA-1) (Platelet-endothelial tetraspan antigen 3) (PETA-3) (Tetraspanin-24) (Tspan-24) (CD antigen CD151)	CD151
P13987	CD59_HUMAN	CD59 glycoprotein (1F5 antigen) (20 kDa homologous restriction factor) (HRF-20) (HRF20) (MAC-inhibitory protein) (MAC-IP) (MEM43 antigen) (Membrane attack complex inhibition factor) (MACIF) (Membrane inhibitor of reactive lysis) (MIRL) (Protectin) (CD antigen CD59)	CD59
P08962	CD63_HUMAN	CD63 antigen (Granulophysin) (Lysosomal-associated membrane protein 3) (LAMP-3) (Melanoma-associated antigen ME491) (OMA81H) (Ocular melanoma-associated antigen) (Tetraspanin-30) (Tspan-30) (CD antigen CD63)	CD63
P60953	CDC42_HUMAN	Cell division control protein 42 homolog (G25K GTP-binding protein)	CDC42
P19022	CADH2_HUMAN	Cadherin-2 (CDw325) (Neural cadherin) (N-cadherin) (CD antigen CD325)	CDH2
Q99653	CHP1_HUMAN	Calcineurin B homologous protein 1 (Calcineurin B-like protein) (Calcium-binding protein CHP) (Calcium-binding protein p22) (EF-hand calcium-binding domain-containing protein p22)	CHP1
P32297	ACHA3_HUMAN	Neuronal acetylcholine receptor subunit alpha-3	CHRNA3
Q9NY35	CLDN1_HUMAN	Claudin domain-containing protein 1 (Membrane protein GENX-3745)	CLDND1
Q9Y696	CLIC4_HUMAN	Chloride intracellular channel protein 4 (Intracellular chloride ion channel protein p64H1)	CLIC4
Q00610	CLH1_HUMAN	Clathrin heavy chain 1 (Clathrin heavy chain on chromosome 17) (CLH-17)	CLTC
P78310	CXAR_HUMAN	Coxsackievirus and adenovirus receptor (CAR) (hCAR) (CVB3-binding protein) (Coxsackievirus B-adenovirus receptor) (HCVADR)	CXADR
O95886	DLGP3_HUMAN	Disks large-associated protein 3 (DAP-3) (PSD-95/SAP90-binding protein 3) (SAP90/PSD-95-associated protein 3) (SAPAP3)	DLGAP3
Q12959	DLG1_HUMAN	Disks large homolog 1 (Synapse-associated protein 97) (SAP-97) (SAP97) (hDlg)	DLG1
P00533	EGFR_HUMAN	Epidermal growth factor receptor (EC 2.7.10.1) (Proto-oncogene c-ErbB-1) (Receptor tyrosine-protein kinase erbB-1)	EGFR
P06733	ENOA_HUMAN	Alpha-enolase (EC 4.2.1.11) (2-phospho-D-glycerate hydro-lyase) (C-myc promoter-binding protein) (Enolase 1) (MBP-1) (MPB-1) (Non-neural enolase) (NNE) (Phosphopyruvate hydratase)	ENO1

		(Plasminogen-binding protein)	
P30040	ERP29_HUMAN	Endoplasmic reticulum resident protein 29 (ERp29) (Endoplasmic reticulum resident protein 28) (ERp28) (Endoplasmic reticulum resident protein 31) (ERp31)	ERP29
Q9BS26	ERP44_HUMAN	Endoplasmic reticulum resident protein 44 (ER protein 44) (ERp44) (Thioredoxin domain-containing protein 4)	ERP44
Q96A65	EXOC4_HUMAN	Exocyst complex component 4 (Exocyst complex component Sec8)	EXOC4
P15311	EZRI_HUMAN	Ezrin (Cytovillin) (Villin-2) (p81)	EZR
Q9H0 × 4	F234A_HUMAN	Protein FAM234A (Protein ITFG3)	FAM234A
Q96AC1	FERM2_HUMAN	Fermitin family homolog 2 (Kindlin-2) (Mitogen-inducible gene 2 protein) (MIG-2) (Pleckstrin homology domain-containing family C member 1) (PH domain-containing family C member 1)	FERMT2
P63096	GNAI1_HUMAN	Guanine nucleotide-binding protein G(i) subunit alpha-1 (Adenylate cyclase-inhibiting G alpha protein)	GNAI1
P08754	GNAI3_HUMAN	Guanine nucleotide-binding protein G(k) subunit alpha (G(i) alpha-3)	GNAI3
P00505	AATM_HUMAN	Aspartate aminotransferase, mitochondrial (mAspAT) (EC 2.6.1.1) (EC 2.6.1.7) (Fatty acid-binding protein) (FABP-1) (Glutamate oxaloacetate transaminase 2) (Kynurenine aminotransferase 4) (Kynurenine aminotransferase IV) (Kynurenine--oxoglutarate transaminase 4) (Kynurenine--oxoglutarate transaminase IV) (Plasma membrane-associated fatty acid-binding protein) (FABPpm) (Transaminase A)	GOT2
Q8TCT9	HM13_HUMAN	Minor histocompatibility antigen H13 (EC 3.4.23.-) (Intramembrane protease 1) (IMP-1) (IMPAS-1) (hIMP1) (Presenilin-like protein 3) (Signal peptide peptidase)	HM13
P09429	HMGB1_HUMAN	High mobility group protein B1 (High mobility group protein 1) (HMG-1)	HMGB1
Q00839	HNRPU_HUMAN	Heterogeneous nuclear ribonucleoprotein U (hnRNP U) (GRIP120) (Nuclear p120 ribonucleoprotein) (Scaffold-attachment factor A) (SAF-A) (p120) (pp120)	HNRNPU
P08238	HS90B_HUMAN	Heat shock protein HSP 90-beta (HSP 90) (Heat shock 84 kDa) (HSP 84) (HSP84)	HSP90AB1
P11021	BIP_HUMAN	Endoplasmic reticulum chaperone BiP (EC 3.6.4.10) (78 kDa glucose-regulated protein) (GRP-78) (Binding-immunoglobulin protein) (BiP) (Heat shock protein 70 family protein 5) (HSP70 family protein 5) (Heat shock protein family A member 5) (Immunoglobulin heavy chain-binding protein)	HSPA5
P10809	CH60_HUMAN	60 kDa heat shock protein, mitochondrial (EC 3.6.4.9) (60 kDa chaperonin) (Chaperonin 60) (CPN60) (Heat shock protein 60) (HSP-60) (Hsp60) (HuCHA60) (Mitochondrial matrix protein P1) (P60 lymphocyte protein)	HSPD1
P11717	MPRI_HUMAN	Cation-independent mannose-6-phosphate receptor (CI Man-6-P receptor) (CI-MPR) (M6PR) (300 kDa mannose 6-phosphate receptor) (MPR 300) (Insulin-like growth factor 2 receptor) (Insulin-like growth factor II receptor) (IGF-II receptor) (M6P/IGF2 receptor) (M6P/IGF2R) (CD antigen CD222)	IGF2R
O75054	IGSF3_HUMAN	Immunoglobulin superfamily member 3 (IgSF3) (Glu-Trp-Ile EWI motif-containing protein 3) (EWI-3)	IGSF3
P46940	IQGA1_HUMAN	Ras GTPase-activating-like protein IQGAP1 (p195)	IQGAP1
Q6UXK2	ISLR2_HUMAN	Immunoglobulin superfamily containing leucine-rich repeat protein 2 (Leucine-rich repeat domain and immunoglobulin domain-containing axon extension protein)	ISLR2
P56199	ITA1_HUMAN	Integrin alpha-1 (CD49 antigen-like family member A) (Laminin and collagen receptor) (VLA-1) (CD antigen CD49a)	ITGA1

P17301	ITA2_HUMAN	Integrin alpha-2 (CD49 antigen-like family member B) (Collagen receptor) (Platelet membrane glycoprotein Ia) (GPIa) (VLA-2 subunit alpha) (CD antigen CD49b)	ITGA2
P06756	ITAV_HUMAN	Integrin alpha-V (Vitronectin receptor) (Vitronectin receptor subunit alpha) (CD antigen CD51) [Cleaved into: Integrin alpha-V heavy chain; Integrin alpha-V light chain]	ITGAV
P05556	ITB1_HUMAN	Integrin beta-1 (Fibronectin receptor subunit beta) (Glycoprotein IIa) (GPIIA) (VLA-4 subunit beta) (CD antigen CD29)	ITGB1
Q12809	KCNH2_HUMAN	Potassium voltage-gated channel subfamily H member 2 (Eag homolog) (Ether-a-go-go-related gene potassium channel 1) (ERG-1) (Eag-related protein 1) (Ether-a-go-go-related protein 1) (H-ERG) (hERG-1) (hERG1) (Voltage-gated potassium channel subunit Kv11.1)	KCNH2
P32004	L1CAM_HUMAN	Neural cell adhesion molecule L1 (N-CAM-L1) (NCAM-L1) (CD antigen CD171)	L1CAM
P09382	LEG1_HUMAN	Galectin-1 (Gal-1) (14 kDa laminin-binding protein) (HLBP14) (14 kDa lectin) (Beta-galactoside-binding lectin L-14-I) (Galaptin) (HBL) (HPL) (Lactose-binding lectin 1) (Lectin galactoside-binding soluble 1) (Putative MAPK-activating protein PM12) (S-Lac lectin 1)	LGALS1
Q9NUP9	LIN7C_HUMAN	Protein lin-7 homolog C (Lin-7C) (Mammalian lin-seven protein 3) (MALS-3) (Vertebrate lin-7 homolog 3) (Veli-3)	LIN7C
Q15334	L2GL1_HUMAN	Lethal(2) giant larvae protein homolog 1 (LLGL) (DLG4) (Hugl-1) (Human homolog to the D-lgl gene protein)	LLGL1
Q12907	LMAN2_HUMAN	Vesicular integral-membrane protein VIP36 (Glycoprotein GP36b) (Lectin mannose-binding 2) (Vesicular integral-membrane protein 36) (VIP36)	LMAN2
Q8IWT6	LRC8A_HUMAN	Volume-regulated anion channel subunit LRRC8A (Leucine-rich repeat-containing protein 8A) (Swelling protein 1)	LRRC8A
P14174	MIF_HUMAN	Macrophage migration inhibitory factor (MIF) (EC 5.3.2.1) (Glycosylation-inhibiting factor) (GIF) (L-dopachrome isomerase) (L-dopachrome tautomerase) (EC 5.3.3.12) (Phenylpyruvate tautomerase)	MIF
O95297	MPZL1_HUMAN	Myelin protein zero-like protein 1 (Protein zero-related)	MPZL1
O00159	MYO1C_HUMAN	Unconventional myosin-Ic (Myosin I beta) (MMI-beta) (MMIb)	MYO1C
P54920	SNAA_HUMAN	Alpha-soluble NSF attachment protein (SNAP-alpha) (N-ethylmaleimide-sensitive factor attachment protein alpha)	NAPA
P13591	NCAM1_HUMAN	Neural cell adhesion molecule 1 (N-CAM-1) (NCAM-1) (CD antigen CD56)	NCAM1
Q9H4L5	OSBL3_HUMAN	Oxysterol-binding protein-related protein 3 (ORP-3) (OSBP-related protein 3)	OSBPL3
O75781	PALM_HUMAN	Paralemmin-1 (Paralemmin)	PALM
P09619	PGFRB_HUMAN	Platelet-derived growth factor receptor beta (PDGF-R-beta) (PDGFR-beta) (EC 2.7.10.1) (Beta platelet-derived growth factor receptor) (Beta-type platelet-derived growth factor receptor) (CD140 antigen-like family member B) (Platelet-derived growth factor receptor 1) (PDGFR-1) (CD antigen CD140b)	PDGFRB
P30101	PDIA3_HUMAN	Protein disulfide-isomerase A3 (EC 5.3.4.1) (58 kDa glucose-regulated protein) (58 kDa microsomal protein) (p58) (Disulfide isomerase ER-60) (Endoplasmic reticulum resident protein 57) (ER protein 57) (ERp57) (Endoplasmic reticulum resident protein 60) (ER protein 60) (ERp60)	PDIA3
P13667	PDIA4_HUMAN	Protein disulfide-isomerase A4 (EC 5.3.4.1) (Endoplasmic reticulum resident protein 70) (ER protein 70) (ERp70) (Endoplasmic reticulum resident protein 72) (ER protein 72) (ERp-72) (ERp72)	PDIA4
P35232	PHB_HUMAN	Prohibitin	PHB

Q99623	PHB2_HUMAN	Prohibitin-2 (B-cell receptor-associated protein BAP37) (D-prohibitin) (Repressor of estrogen receptor activity)	PHB2
Q13492	PICAL_HUMAN	Phosphatidylinositol-binding clathrin assembly protein (Clathrin assembly lymphoid myeloid leukemia protein)	PICALM
P98161	PKD1_HUMAN	Polycystin-1 (PC1) (Autosomal dominant polycystic kidney disease 1 protein)	PKD1
Q15139	KPCD1_HUMAN	Serine/threonine-protein kinase D1 (EC 2.7.11.13) (Protein kinase C mu type) (Protein kinase D) (nPKC-D1) (nPKC-mu)	PRKD1
Q9NRY6	PLS3_HUMAN	Phospholipid scramblase 3 (PL scramblase 3) (Ca(2+)-dependent phospholipid scramblase 3)	PLSCR3
O15031	PLXB2_HUMAN	Plexin-B2 (MM1)	PLXNB2
P49768	PSN1_HUMAN	Presenilin-1 (PS-1) (EC 3.4.23.-) (Protein S182) [Cleaved into: Presenilin-1 NTF subunit; Presenilin-1 CTF subunit; Presenilin-1 CTF12 (PS1-CTF12)]	PSEN1
Q9P2B2	FPRP_HUMAN	Prostaglandin F2 receptor negative regulator (CD9 partner 1) (CD9P-1) (Glu-Trp-Ile EWI motif-containing protein F) (EWI-F) (Prostaglandin F2-alpha receptor regulatory protein) (Prostaglandin F2-alpha receptor-associated protein) (CD antigen CD315)	PTGFRN
P15151	PVR_HUMAN	Poliovirus receptor (Nectin-like protein 5) (NECL-5) (CD antigen CD155)	PVR
P61026	RAB10_HUMAN	Ras-related protein Rab-10	RAB10
P51153	RAB13_HUMAN	Ras-related protein Rab-13 (Cell growth-inhibiting gene 4 protein)	RAB13
Q9NP72	RAB18_HUMAN	Ras-related protein Rab-18	RAB18
Q15286	RAB35_HUMAN	Ras-related protein Rab-35 (GTP-binding protein RAY) (Ras-related protein Rab-1C)	RAB35
P20339	RAB5A_HUMAN	Ras-related protein Rab-5A	RAB5A
P61006	RAB8A_HUMAN	Ras-related protein Rab-8A (Oncogene c-mel)	RAB8A
P63000	RAC1_HUMAN	Ras-related C3 botulinum toxin substrate 1 (Cell migration-inducing gene 5 protein) (Ras-like protein TC25) (p21-Rac1)	RAC1
P60763	RAC3_HUMAN	Ras-related C3 botulinum toxin substrate 3 (p21-Rac3)	RAC3
P11233	RALA_HUMAN	Ras-related protein Ral-A	RALA
P35241	RADI_HUMAN	Radixin	RDX
O15258	RER1_HUMAN	Protein RER1	RER1
P61586	RHOA_HUMAN	Transforming protein RhoA (Rho cDNA clone 12) (h12)	RHOA
P08134	RHOC_HUMAN	Rho-related GTP-binding protein RhoC (Rho cDNA clone 9) (h9)	RHOC
Q01974	ROR2_HUMAN	Tyrosine-protein kinase transmembrane receptor ROR2 (EC 2.7.10.1) (Neurotrophic tyrosine kinase, receptor-related 2)	ROR2
P62070	RRAS2_HUMAN	Ras-related protein R-Ras2 (Ras-like protein TC21) (Teratocarcinoma oncogene)	RRAS2
Q14108	SCRB2_HUMAN	Lysosome membrane protein 2 (85 kDa lysosomal membrane sialoglycoprotein) (LGP85) (CD36 antigen-like 2) (Lysosome membrane protein II) (LIMP II) (Scavenger receptor class B member 2) (CD antigen CD36)	SCARB2
P18827	SDC1_HUMAN	Syndecan-1 (SYND1) (CD antigen CD138)	SDC1

P53985	MOT1_HUMAN	Monocarboxylate transporter 1 (MCT 1) (Solute carrier family 16 member 1)	SLC16A1
P43007	SATT_HUMAN	Neutral amino acid transporter A (Alanine/serine/cysteine/threonine transporter 1) (ASCT-1) (SATT) (Solute carrier family 1 member 4)	SLC1A4
Q15758	AAAT_HUMAN	Neutral amino acid transporter B(0) (ATB(0)) (Baboon M7 virus receptor) (RD114/simian type D retrovirus receptor) (Sodium-dependent neutral amino acid transporter type 2) (Solute carrier family 1 member 5)	SLC1A5
P08195	4F2_HUMAN	4F2 cell-surface antigen heavy chain (4F2hc) (4F2 heavy chain antigen) (Lymphocyte activation antigen 4F2 large subunit) (Solute carrier family 3 member 2) (CD antigen CD98)	SLC3A2
P23975	SC6A2_HUMAN	Sodium-dependent noradrenaline transporter (Norepinephrine transporter) (NET) (Solute carrier family 6 member 2)	SLC6A2
O14745	NHRF1_HUMAN	Na(+)/H(+) exchange regulatory cofactor NHE-RF1 (NHERF-1) (Ezrin-radixin-moesin-binding phosphoprotein 50) (EBP50) (Regulatory cofactor of Na(+)/H(+) exchanger) (Sodium-hydrogen exchanger regulatory factor 1) (Solute carrier family 9 isoform A3 regulatory factor 1)	SLC9A3R1
P60880	SNP25_HUMAN	Synaptosomal-associated protein 25 (SNAP-25) (Super protein) (SUP) (Synaptosomal-associated 25 kDa protein)	SNAP25
Q99523	SORT_HUMAN	Sortilin (100 kDa NT receptor) (Glycoprotein 95) (Gp95) (Neurotensin receptor 3) (NT3) (NTR3)	SORT1
P12931	SRC_HUMAN	Proto-oncogene tyrosine-protein kinase Src (EC 2.7.10.2) (Proto-oncogene c-Src) (pp60c-src) (p60-Src)	SRC
Q12846	STX4_HUMAN	Syntaxin-4 (Renal carcinoma antigen NY-REN-31)	STX4
O15400	STX7_HUMAN	Syntaxin-7	STX7
Q9Y4C2	TCAF1_HUMAN	TRPM8 channel-associated factor 1 (TRP channel-associated factor 1)	TCAF1
P02786	TFR1_HUMAN	Transferrin receptor protein 1 (TR) (TfR) (TfR1) (Trfr) (T9) (p90) (CD antigen CD71) [Cleaved into: Transferrin receptor protein 1, serum form (sTfR)]	TFRC
P04216	THY1_HUMAN	Thy-1 membrane glycoprotein (CDw90) (Thy-1 antigen) (CD antigen CD90)	THY1
Q9Y490	TLN1_HUMAN	Talin-1	TLN1
P49755	TMEDA_HUMAN	Transmembrane emp24 domain-containing protein 10 (21 kDa transmembrane-trafficking protein) (S31III125) (S31I125) (Tmp-21-I) (Transmembrane protein Tmp21) (p23) (p24 family protein delta-1) (p24delta1) (p24delta)	TMED10
Q9H813	TM206_HUMAN	Transmembrane protein 206	TMEM206
Q96JJ7	TMX3_HUMAN	Protein disulfide-isomerase TMX3 (EC 5.3.4.1) (Thioredoxin domain-containing protein 10) (Thioredoxin-related transmembrane protein 3)	TMX3
Q13641	TPBG_HUMAN	Trophoblast glycoprotein (5T4 oncofetal antigen) (5T4 oncofetal trophoblast glycoprotein) (5T4 oncotrophoblast glycoprotein) (M6P1) (Wnt-activated inhibitory factor 1) (WAIF1)	TPBG
Q8NG11	TSN14_HUMAN	Tetraspanin-14 (Tspan-14) (DC-TM4F2) (Transmembrane 4 superfamily member 14)	TSPAN14
P54578	UBP14_HUMAN	Ubiquitin carboxyl-terminal hydrolase 14 (EC 3.4.19.12) (Deubiquitinating enzyme 14) (Ubiquitin thioesterase 14) (Ubiquitin-specific-processing protease 14)	USP14
Q15836	VAMP3_HUMAN	Vesicle-associated membrane protein 3 (VAMP-3) (Cellubrevin) (CEB) (Synaptobrevin-3)	VAMP3
P51809	VAMP7_HUMAN	Vesicle-associated membrane protein 7 (VAMP-7) (Synaptobrevin-like protein 1) (Tetanus-insensitive VAMP) (Ti-VAMP)	VAMP7

Q9P0L0	VAPA_HUMAN	Vesicle-associated membrane protein-associated protein A (VAMP-A) (VAMP-associated protein A) (VAP-A) (33 kDa VAMP-associated protein) (VAP-33)	VAPA
P21796	VDAC1_HUMAN	Voltage-dependent anion-selective channel protein 1 (VDAC-1) (hVDAC1) (Outer mitochondrial membrane protein porin 1) (Plasmalemmal porin) (Porin 31HL) (Porin 31HM)	VDAC1

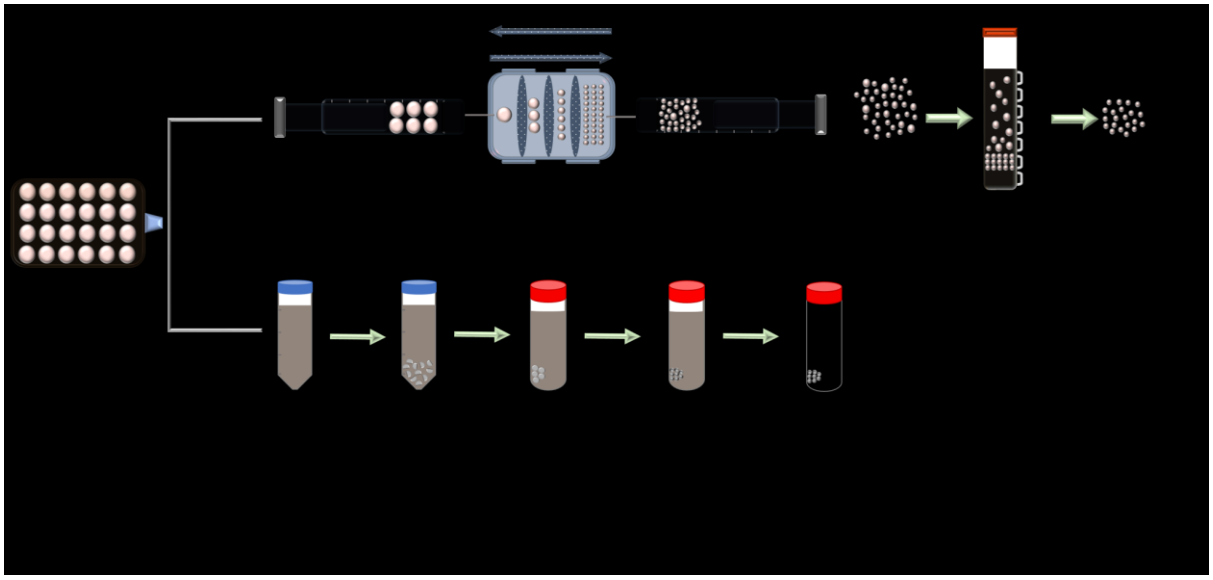

Figure 2

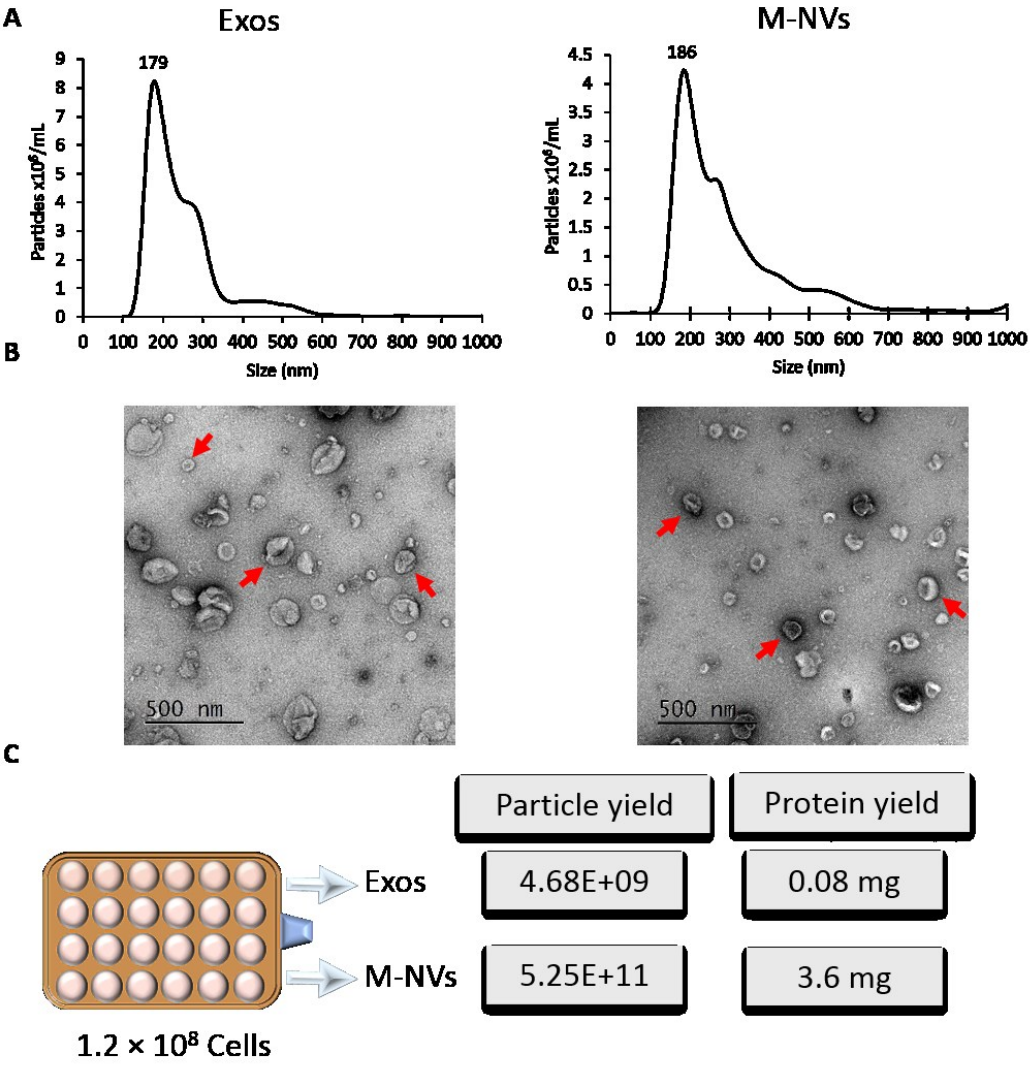

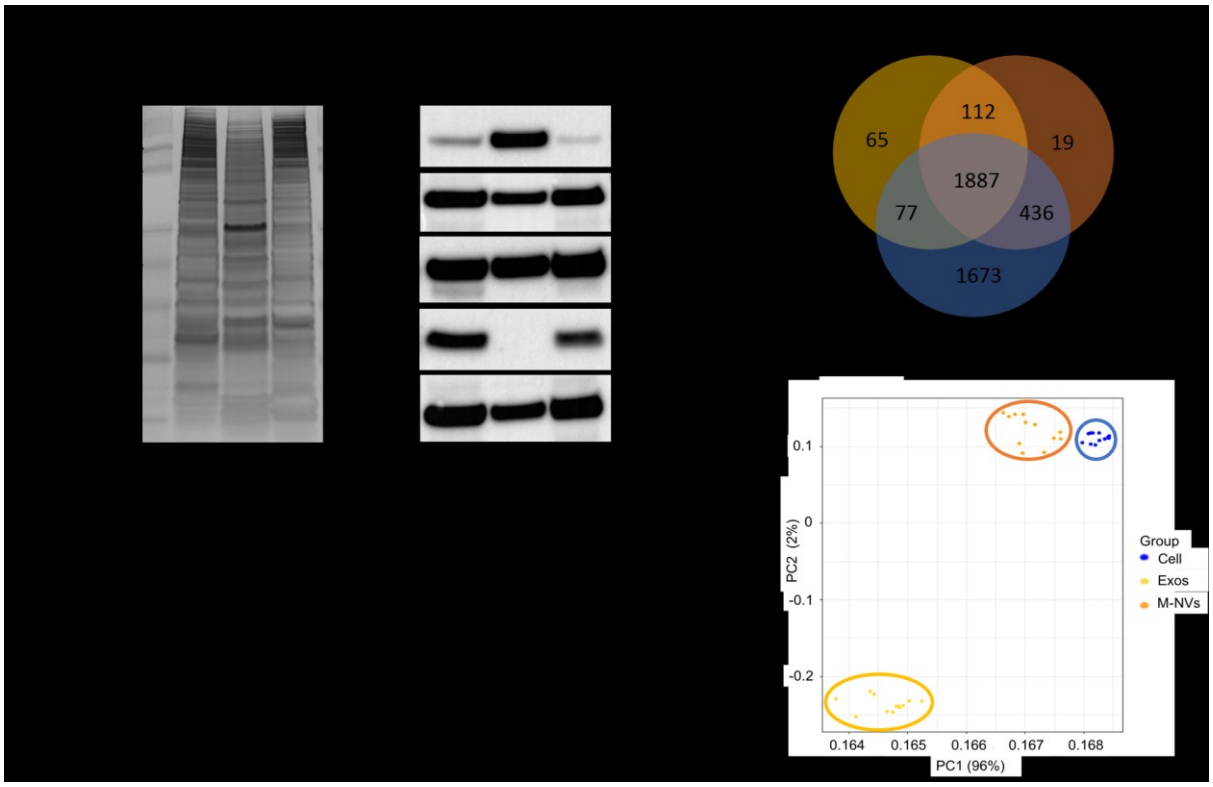

Figure 4